Electronic Supplementary Material (ESI) for Polymer Chemistry.

A general route to chiral nanostructures from helical polymers: P/M switch via dynamic metal coordination

Sandra Arias, Manuel Núñez-Martínez, Emilio Quiñoá, Ricardo Riguera* and Félix Freire*

Centro Singular de Investigación en Química Biolóxica e Materiais Moleculares (CIQUS) and Departmento de Química Orgánica, Universidade de Santiago de Compostela, 15782 Santiago de Compostela, Spain

ricardo.riguera@usc.es, felix.freire@usc.es

http://www.usc.es/gi1608/

Electronic Supporting Information

Contents

Structures and codes

Monomer	**Polymer**
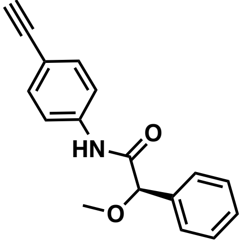	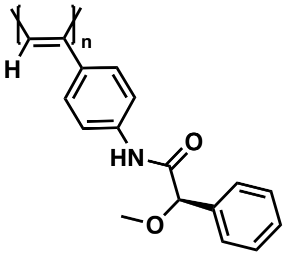
M**1**	Poly-(*R*)-**1**
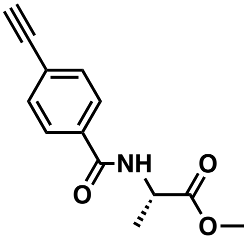	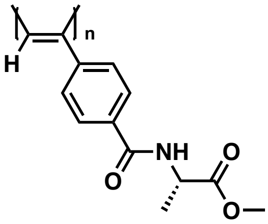
M**2**	Poly-**2**
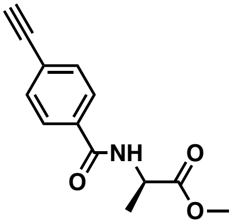	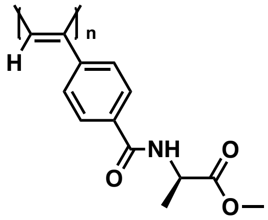
M**3**	Poly-**3**
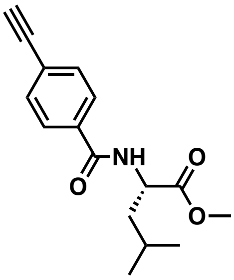	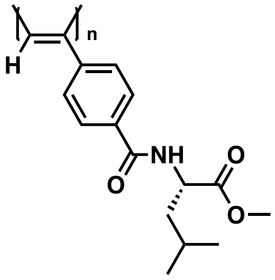
M**4**	Poly-**4**
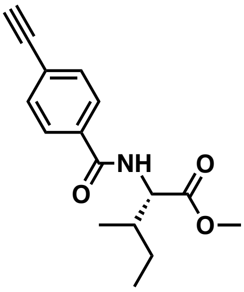	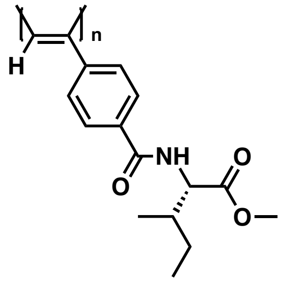
M**5**	Poly-**5**

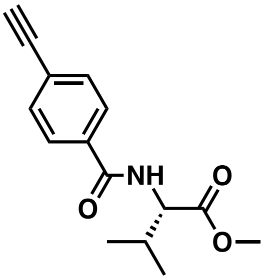	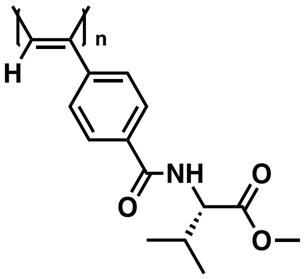
M**6**	Poly-**6**

1. Synthesis of monomers and polymers

The general procedure for the synthesis of monomer M**1** and polymer poly-(*R*)-**1** (Figure S1) can be found in reference [i].

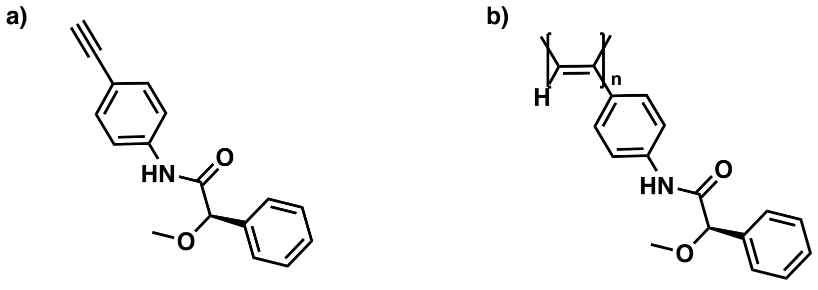

M**1** poly-(*R*)-**1**

Figure S1: Structures of (a) (*R*)-MPA monomer M**1** and (b) poly-(*R*)-**1**.

1.1 Synthesis of monomers

- **Synthesis and data of monomer M2.**

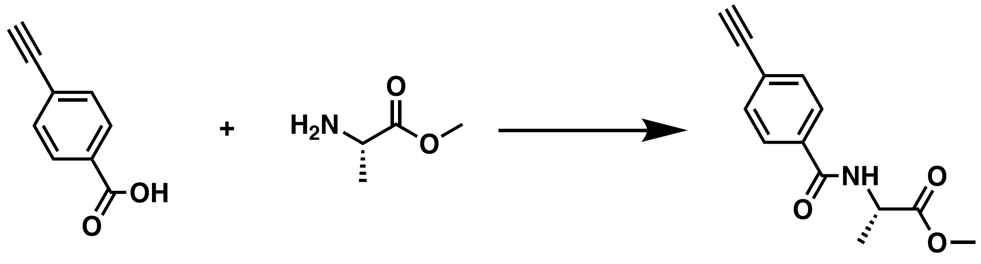

1 **2** M**2**

1-Ethyl-3-(3-dimethylaminopropyl)carbodiimide (EDC, 1.350 g, 1.2 equiv.), hydroxybenzotriazole (HOBt, 1.400 g, 1.2 equiv.), 2-ethynylbenzoic acid (1.700 g, 1.2 equiv) and diisopropyltriethylamine (DIPEA, 1 mL, 2.0 equiv.) were dissolved in 70 mL of CH_2Cl_2, and the mixture was stirred for 15 min to activate the acid. Then, methyl *L*-alaninate (1.151 g, 1.0 equiv) was added and the reaction mixture was stirred overnight. The organic layer was washed with HCl 1M, saturated solution of $NaHCO_3$ and brine. The combined organic layers were dried over anhyd Na_2SO_4, filtered and the solvent was evaporated at reduced pressure. The crude product was chromatographed on silica gel (70-230 mesh) with hexane/ethyl acetate (7/3) as eluent [2.112 g M**2**], 82% of pure product.

Spectroscopic data:

^{1}H NMR (300 MHz, $CDCl_3$) δ (ppm): 1.49 (d, 3H), 3.25 (s, 1H), 3.74 (s, 3H), 4.75 (q, 1H), 7.29 (d, 1H), 7.48 (d, 2H), 7.76 (d, 2H).

^{13}C NMR (75 MHz, $CDCl_3$) δ (ppm): 18.0, 48.5, 52.4, 79.7, 82.7, 125.4, 127.1, 132.0, 133.6, 166.2, 173.5.
[α]$_D$= +81 (15 mg mL^{-1}, $CHCl_3$)

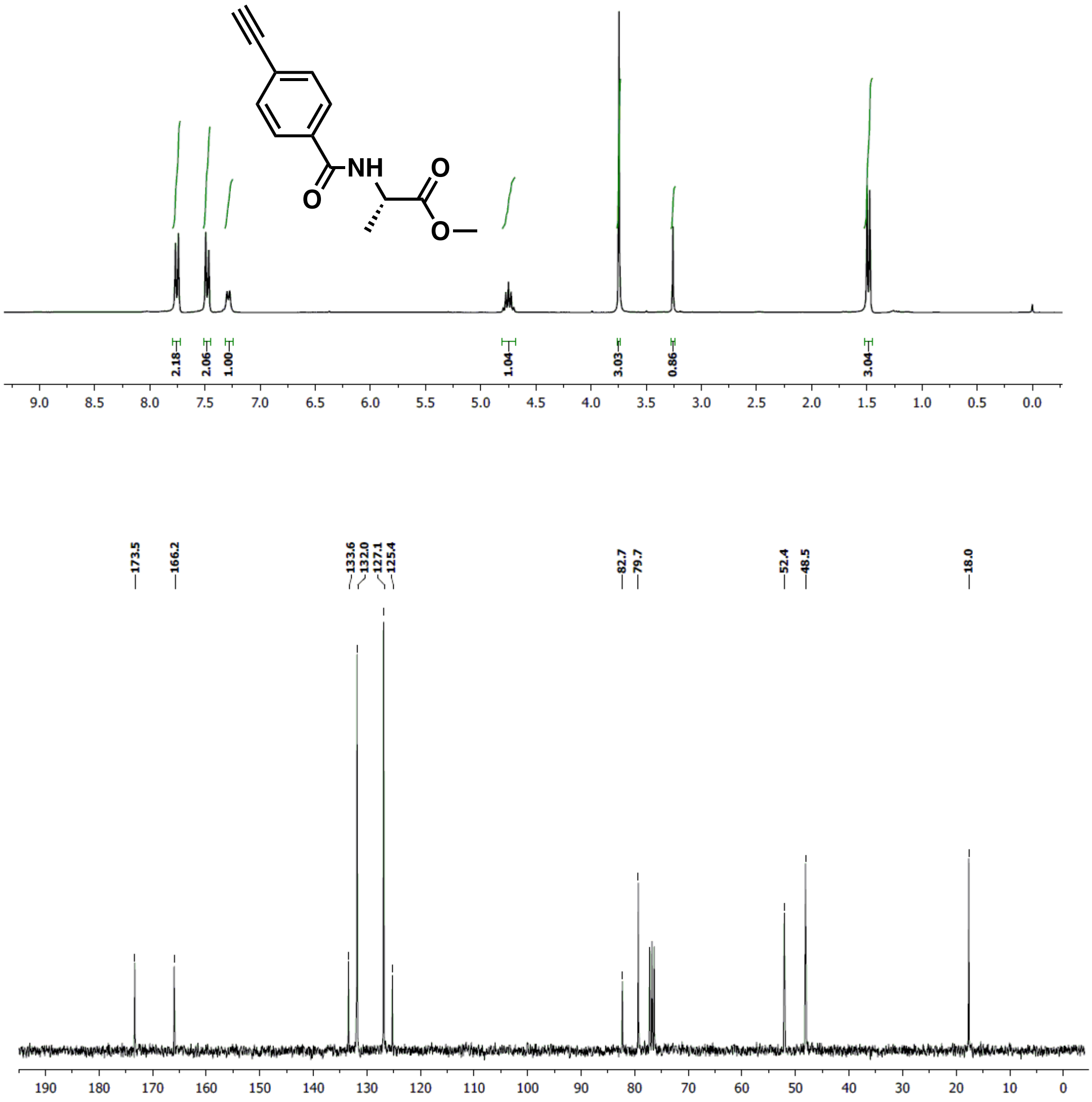

Figure S2: ^{1}H- and ^{13}C-NMR spectra of M**2**.

- **Synthesis and data of monomer M3.**

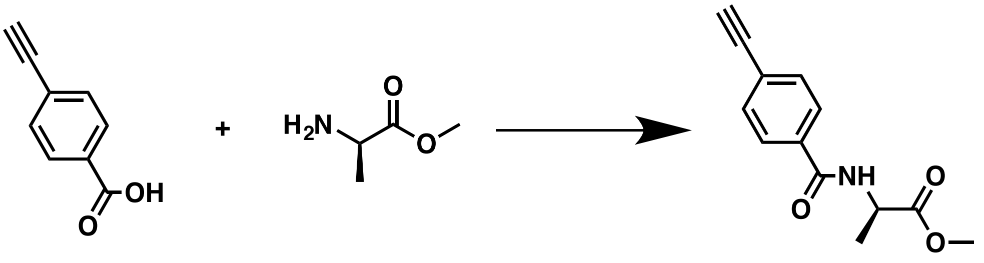

1 **3** M**3**

1-Ethyl-3-(3-dimethylaminopropyl)carbodiimide (EDC, 1.350 g, 1.2 equiv.), hydroxybenzotriazole (HOBt, 1.400 g, 1.2 equiv), 2-ethynylbenzoic acid (1.700 g, 1.2 equiv) and diisopropyltriethylamine (DIPEA, 1 mL, 2.0 equiv) were dissolved in 70 mL of CH_2Cl_2, and the mixture was stirred for 15 min to activate the acid. Then, methyl *D*-alaninate (1.000 g, 1.0 equiv) was added and the reaction mixture was stirred overnight. The organic layer was washed with HCl 1M, saturated solution of $NaHCO_3$ and brine. The combined organic layers were dried over anhyd Na_2SO_4, filtered and the solvent was evaporated at reduced pressure. The crude product was chromatographed on silica gel (70-230 mesh) with hexane/ethyl acetate (7/3) as eluent [1.771 g M**3**], 79% of pure product.

Spectroscopic data:

^{1}H NMR (300 MHz, $CDCl_3$) δ (ppm): 1.52 (d, 3H), 3.19 (s,1H), 3.78 (s, 3H), 4.77 (q,1H), 6.80 (d, 1H), 7.52 (d, 2H), 7.73 (d, 2H).

^{13}C NMR (75 MHz, $CDCl_3$) δ (ppm): 18.7, 48.6, 52.8, 79.8, 82.8, 125.7, 127.1, 132.4, 133.9, 165.9, 173.7.

$[\alpha]_D$= -76 (15 mg mL^{-1}, $CHCl_3$)

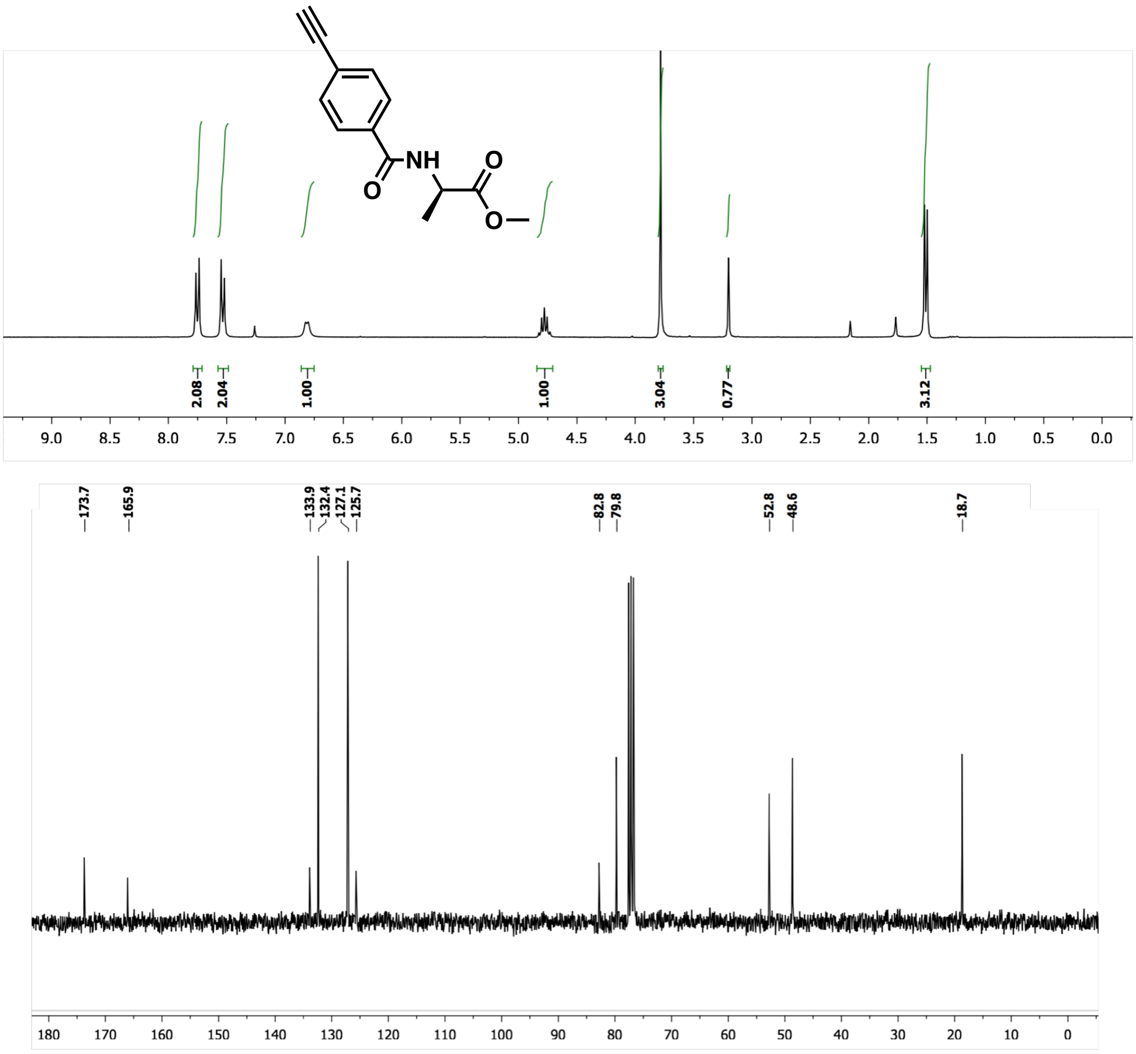

Figure S3: ^{1}H- and ^{13}C-NMR spectra of M**3**.

- **Synthesis and data of monomer M4**

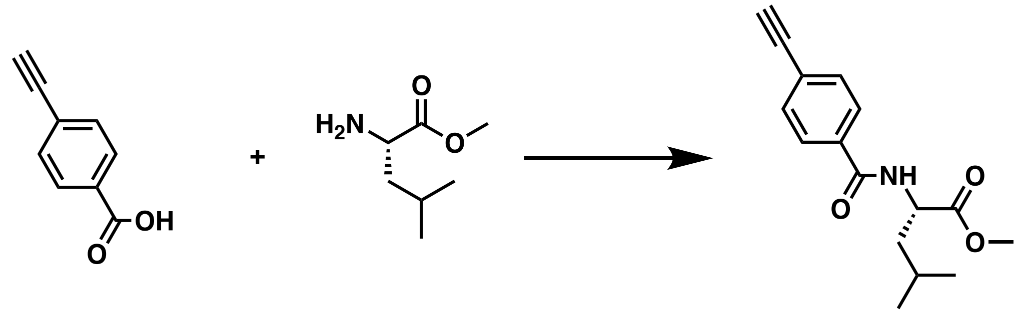

1 **4** M**4**

1-Ethyl-3-(3-dimethylaminopropyl)carbodiimide (EDC, 0.122 g, 1.2 equiv.), hydroxybenzotriazole (HOBt, 0.087 g, 1.2 equiv), 2-ethynylbenzoic acid (1.7 g, 1.2 equiv) and diisopropyltriethylamine (DIPEA, 111 μL, 2.0 equiv) were dissolved in 30 mL of CH_2Cl_2, and the mixture was stirred for 15 min to activate the acid. Then, methyl *L*-leucinate (0.771 g, 1.0 equiv) was added and the reaction mixture was stirred overnight. The organic layer was washed with HCl 1M, saturated solution of $NaHCO_3$ and brine. The combined organic layers were dried over anhyd Na_2SO_4, filtered and the solvent was evaporated at reduced pressure. The crude product was chromatographed on silica gel (70-230 mesh) with hexane/ethyl acetate (7/3) as eluent [1.001 g M**4**], 69% of pure product.

Spectroscopic data:

^{1}H NMR (300 MHz, $CDCl_3$) δ (ppm): 0.94 (d, 6H), 1.73 (m, 3H), 3.29 (s, 1H), 3.73 (s, 3H), 4.81 (q, 1H), 7.43 (d, 2H), 7.58 (d, 1H), 7.74 (d, 2H).

^{13}C NMR (75 MHz, $CDCl_3$) δ (ppm): 21.6, 22.8, 24.9, 29.5, 40.8, 51.2, 52.2, 70.8, 82.7, 125.5, 127.1, 131.9, 133.5, 166.6, 173.8.

$[\alpha]_D$ = +44 (15 mg mL^{-1}, $CHCl_3$)

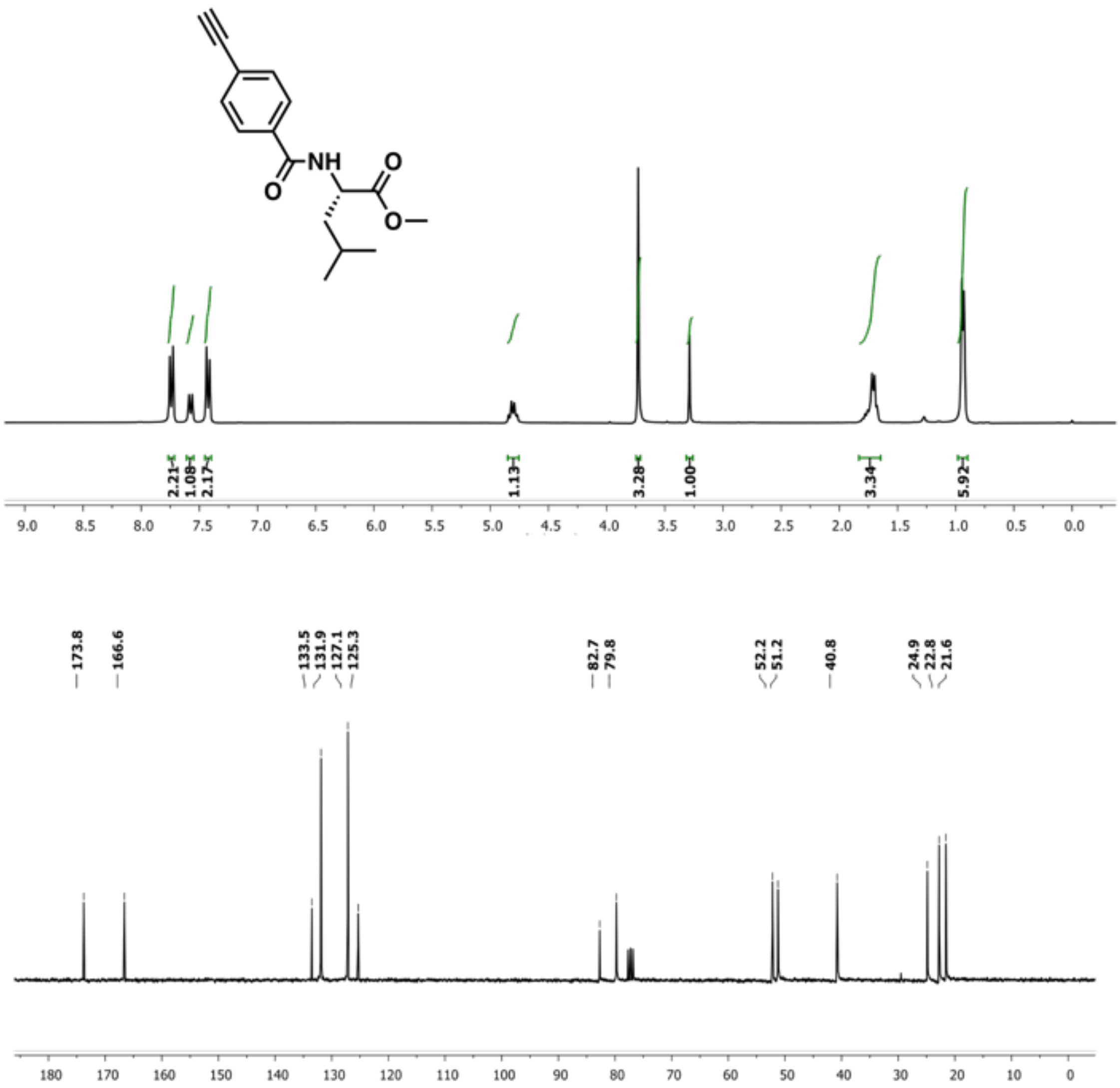

Figure S4: ^{1}H- and ^{13}C-NMR spectra of M**4**.

- **Synthesis and data of monomer M5**

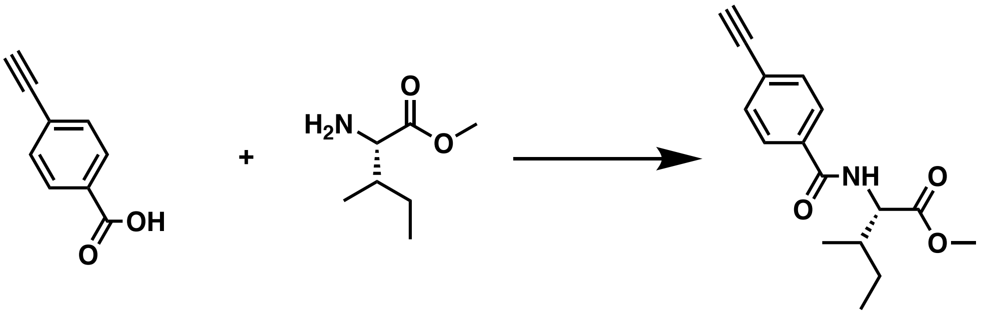

1 **5** M**5**

1-Ethyl-3-(3-dimethylaminopropyl)carbodiimide (EDC, 1.350 g, 1.2 equiv.), hydroxybenzotriazole (HOBt, 1.400 g, 1.2 equiv), 2-ethynylbenzoic acid (1.700 g, 1.2 equiv) and diisopropyltriethylamine (DIPEA, 1 ml, 2.0 equiv) were dissolved in 70 mL of CH_2Cl_2, and the mixture was stirred for 15 min to activate the acid. Then, methyl *L*-isoleucinate (1.151 g, 1.0 equiv) was added and the reaction mixture was stirred overnight. The organic layer was washed with HCl 1M, saturated solution of $NaHCO_3$ and brine. The combined organic layers were dried over anhyd Na_2SO_4, filtered and the solvent was evaporated at reduced pressure. The crude product was chromatographed on silica gel (70-230 mesh) with hexane/ethyl acetate (7/3) as eluent [1.550 g M**5**], 72% of pure product

Spectroscopic data:
^{1}H NMR (300 MHz, $CDCl_3$) δ (ppm): 0.87 (d, 6H), 1.18 (m, 2H), 1.44 (m, 1H), 1.92 (m, 1H), 3.18 (s, 1H), 3.67 (s, 3H), 4.68 (t, 1H), 6.91 (d, 1H), 7.40 (d, 2H), 7.66 (d, 2H).
^{13}C NMR (75 MHz, $CDCl_3$) δ (ppm): 11.3, 15.3, 25.2, 37.8, 51.9, 56.8, 79.6, 82.5, 125.3, 126.9, 131.9, 133.8, 166.2, 172.4.
$[\alpha]_D = +74$ (15 mg mL^{-1}, $CHCl_3$).

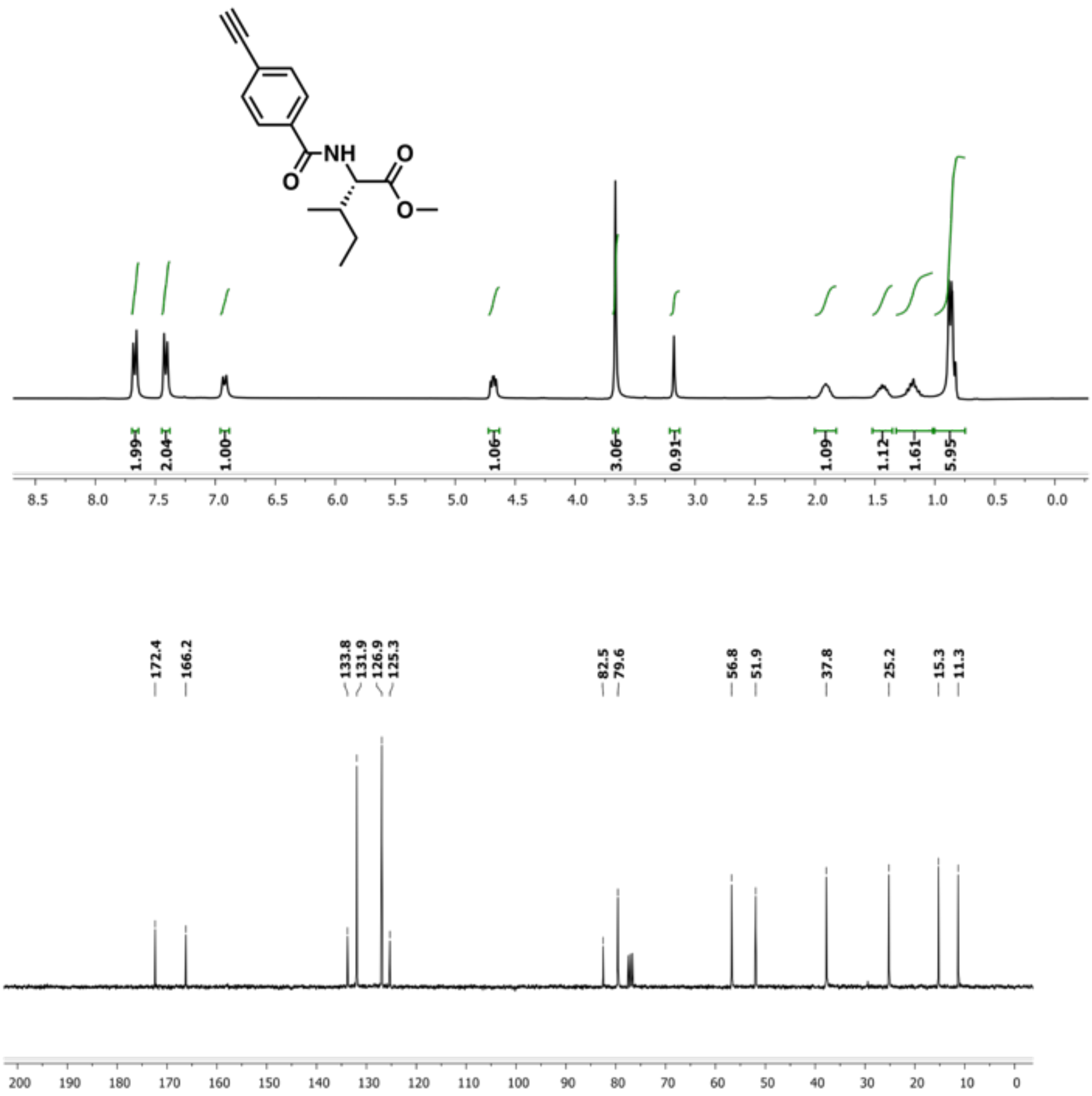

Figure S5: ^{1}H- and ^{13}C-NMR spectra of M**5**.

- **Synthesis and data of monomer M6**

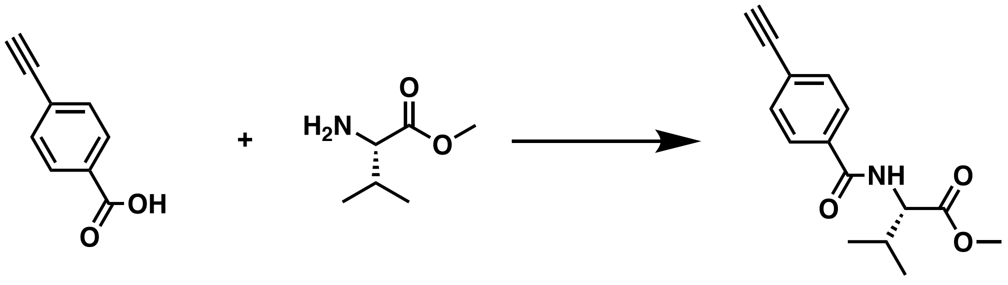

1 **6** M**6**

1-Ethyl-3-(3-dimethylaminopropyl)carbodiimide (EDC, 0.656, 1.2 equiv.), hydroxybenzotriazole (HOBt, 0.465 g, 1.2 equiv), 2-ethynylbenzoic acid (0.500 g, 1.2 equiv) and diisopropyltriethylamine (DIPEA, 695 mL, 2.0 equiv) were dissolved in 50 mL of CH_2Cl_2, and the mixture was stirred for 15 min to activate the acid. Then, methyl *L*-valinate (0.398 g, 1.0 equiv) was added and the reaction mixture was stirred overnight. The organic layer was washed with HCl 1M, saturated solution of $NaHCO_3$ and brine. The combined organic layers were dried over anhyd Na_2SO_4, filtered and the solvent was evaporated at reduced pressure. The crude product was chromatographed on silica gel (70-230 mesh) with hexane/ethyl acetate (7/3) as eluent [0.597 g M**6**], 75% of pure product.

Spectroscopic data:

^{1}H NMR (300 MHz, $CDCl_3$) δ (ppm): 0.96 (m, 6H), 2.24 (m, 1H), 3.19 (1H, s), 3.73 (3H, s), 4.72 (q, 1H), 6.73 (d, 1H), 7.50 (d, 2H), 7.73 (d, 2H).

^{13}C NMR (75 MHz, $CDCl_3$) δ (ppm): 18.1, 19.0, 31.6, 52.3, 71.3, 79.7, 82.8, 125.6, 127.1, 132.3, 134.1, 166.5, 172.6

$[\alpha]_D$= +36 (15 mg mL^{-1}, $CHCl_3$)

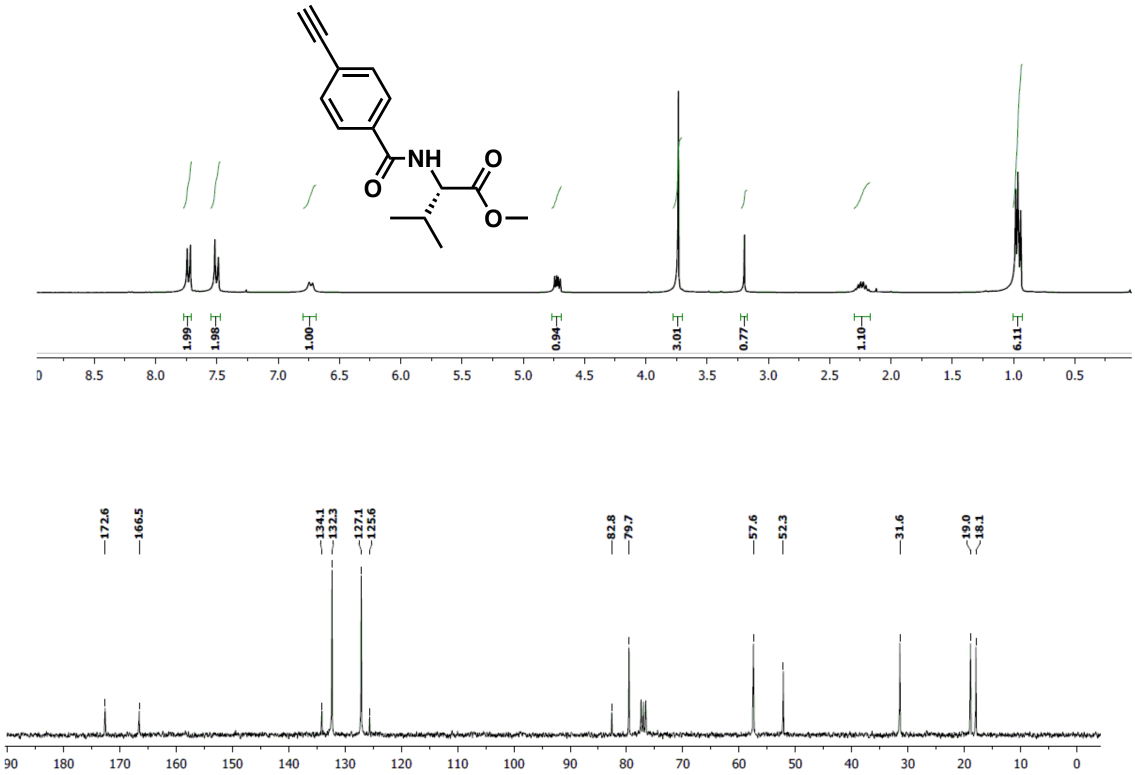

Figure S6: ^{1}H- and ^{13}C NMR spectra of monomer M**6**.

1.2 Synthesis of polymers

The polymers were synthesized in a reaction flask (sealed ampoule) that was dried under vacuum and flushed with argon for three times before monomers were added as a solid. Then, the flask was evacuated on a vacuum line and flushed with dry argon (three times). Dry THF was added with a syringe and then, Et_3N dropwise. A solution of rhodium norbornadiene chloride dimer, $[Rh(nbd)Cl]_2$, in THF was added at 30 °C. The reaction mixture was stirred at 30 °C for 24 h. Next, the resulting polymers were diluted in CH_2Cl_2 and they were precipitated in a large amount of diethyl ether, centrifuged (twice) and re-precipitated in hexane and centrifuged again.

Monomer	**Mass(mg)**	**THF(μL)**	**Et_3N (μL)**	**Catalyst (mg)**	**Yield (%)**
Poly-**2**	100	1000	5	2	88
Poly-**3**	100	1000	5	2	87
Poly-**4**	100	1000	5	2	90
Poly-**5**	100	1000	5	2	98
Poly-**6**	100	1000	5	2	89

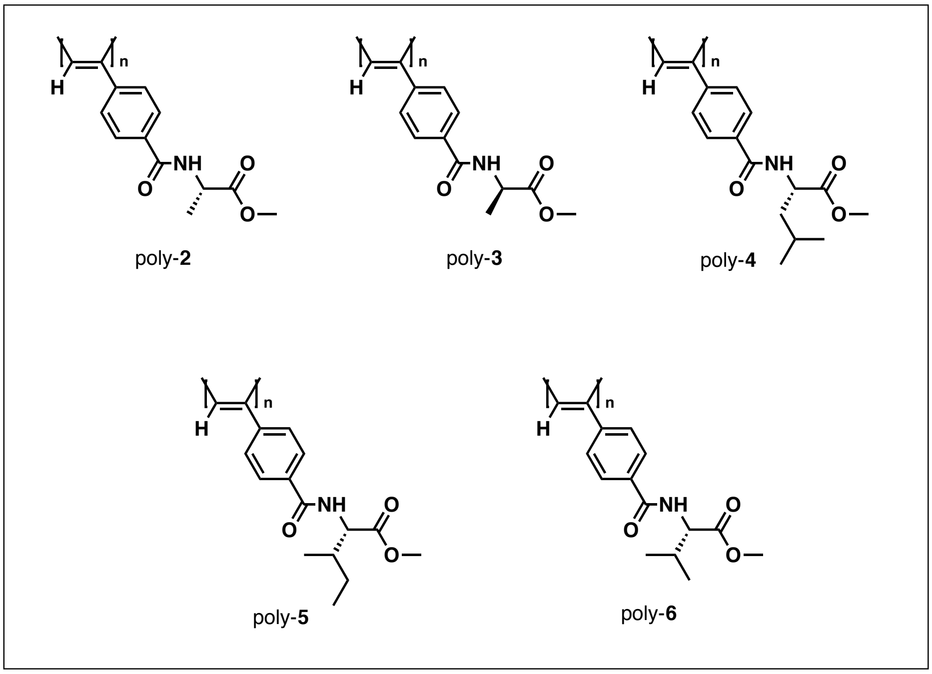

poly-**2** poly-**3** poly-**4** poly-**5** poly-**6**

The *cis* stereoregularity of the polymers was determined by ^{1}H-NMR spectroscopy (Figure S7a, c, e, g, i) where the vinyl proton resonates at 5.8 ppm, and Raman resonances (Figure S7b, d, f, h, j). The peak at 1610-1570 cm^{-1} is assigned to C=C bond stretching in the *cis* poly(acetylene) and overlaps with that of the phenyl ring. The peak at 1350-1340 cm^{-1} is assigned to the *cis* C-C bond coupled with the single bond connecting the main chain and the phenyl ring. The peak at 1010-960 cm^{-1} is assigned to the C-H bond deformation of the *cis* form.

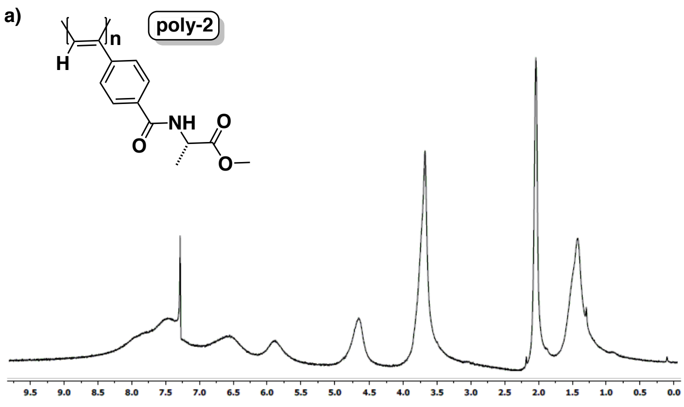

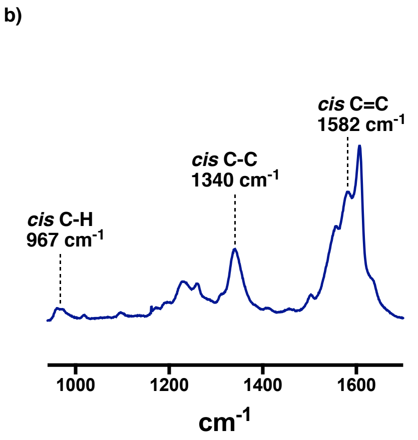

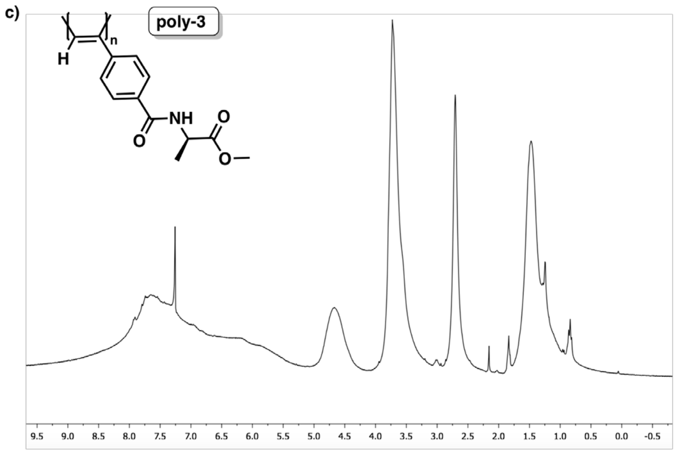

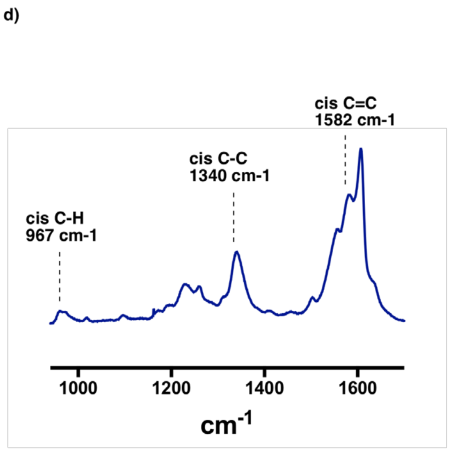

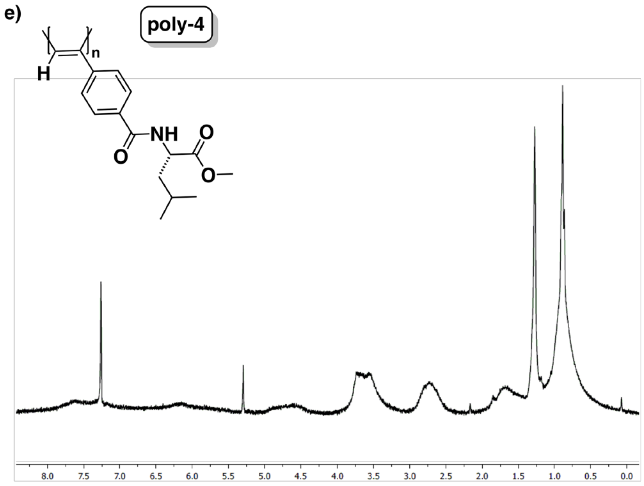

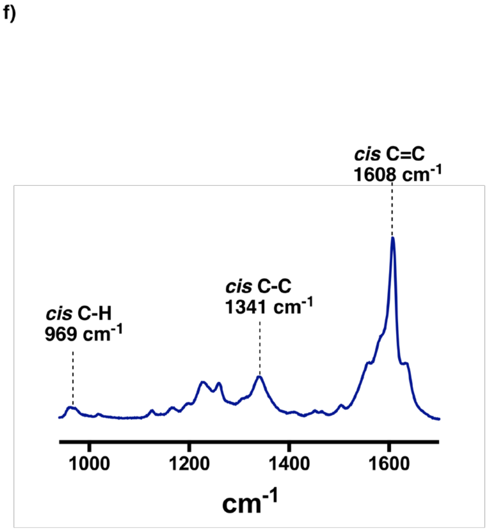

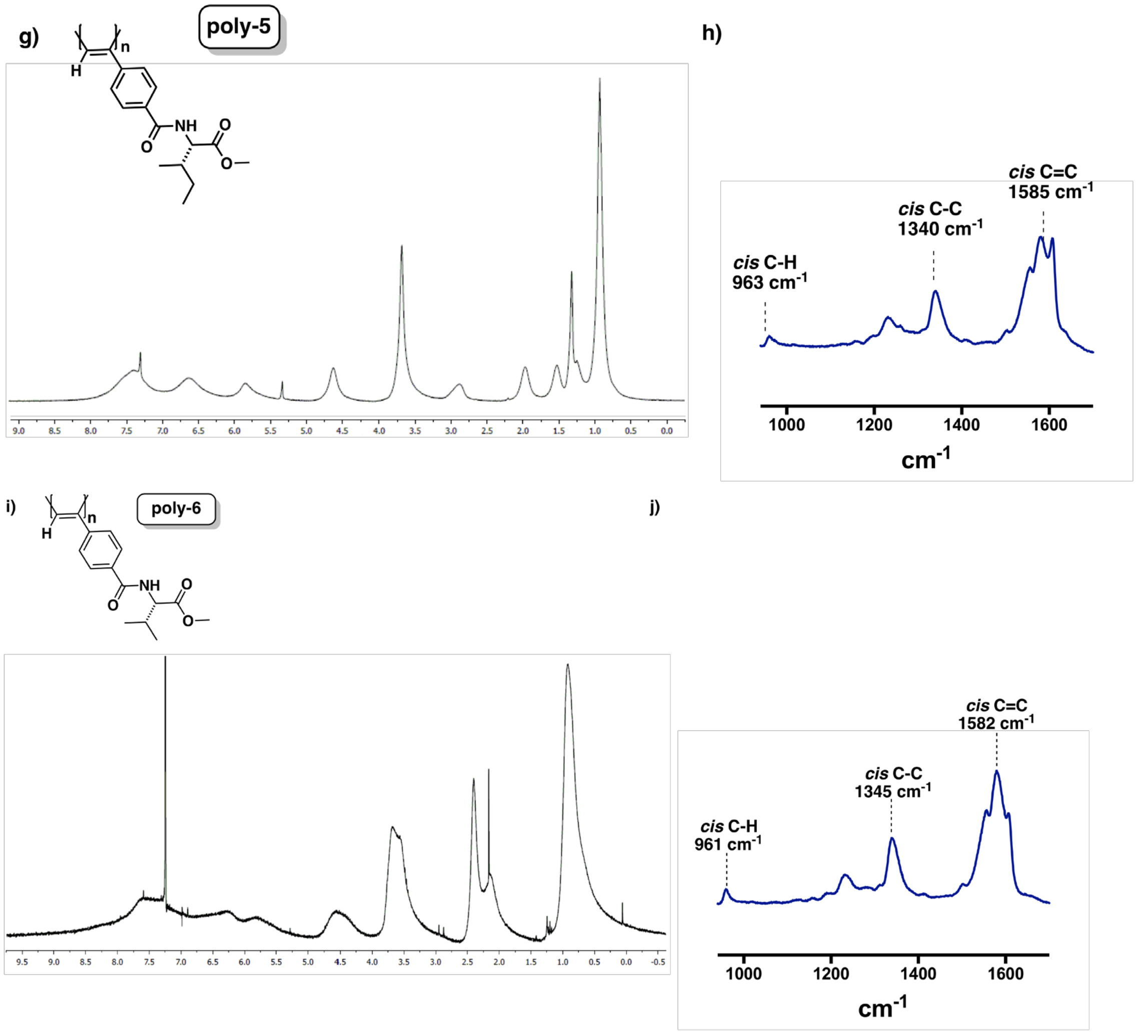

Figure S7: ^{1}H NMR and raman spectra of: a-b) poly-**2**, c-d) poly-**3**, e-f) poly-**4**, g-h) poly-**5**, i-j) poly-**6**.

GPC studies

GPC data were obtained in an Aliance 2695 HPLC with a UV-2489 detector (Waters). The samples were eluted by three Phenogel columns connected to each other with stationary phases of 10^3, 10^4 and 10^5 Armstrong and packed with a solid support of a cross-linked styrene and *p*-divinylbenzene copolymer. GPC data of the polymers for this manuscript see the table below.

Table S1: GPC data of poly-**2**, poly-**3**, poly-**4**, poly-**5**, poly-**6**:

Polymer	Mn	Mw	Mp	Mz	Mz/Mw
poly-**2**	20823	54320	84477	106053	1.95
poly-**3**	11469	22815	18817	55395	2.42
poly-**4**	30902	247118	449082	588863	2.38
poly-**5**	45377	129203	162848	261554	2.02
poly-**6**	45297	170013	172184	374847	2.20

2. Thermal studies

DSC studies

DSC traces were obatined in a DSC Q200 Txero Technology (TA instruments, New Castle, UK), equipped with a refrigerated cooling system RCS90 (TA Instruments, New Castle, UK), using a Tzero low-mass aluminum pan.

DSC studies were carried out in order to determine de geometry of the polymer backbone. As a general protocol, a polymer sample was kept in an aluminum pan and heated from 40 °C to 350 °C with a heating rate of 10 °C/min (Figure S8).

The thermograms of the polymers show typical traces for a *cis-trans* backbone, where two exothermal peaks corresponding to the *c-t* to *c-c* and the *c-c* to *t-t* were observed.

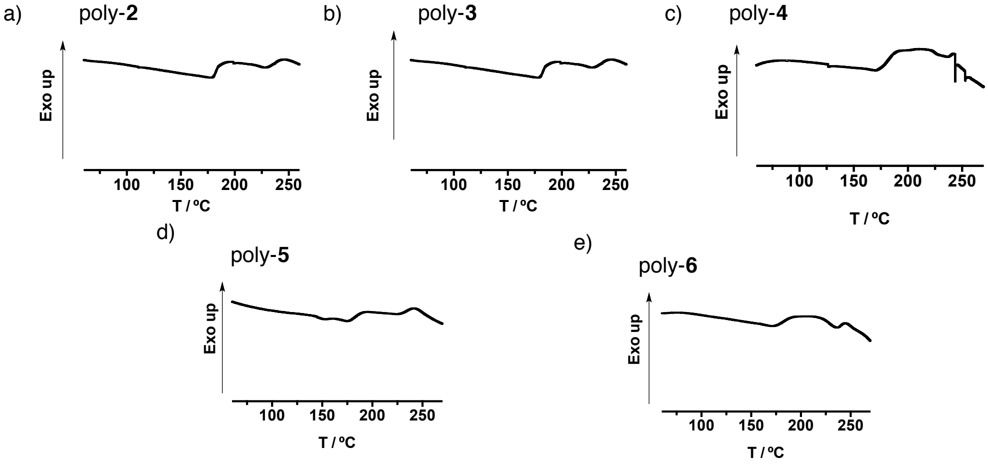

Figure S8: DSC thermograms of a) poly-**2**, b) poly-**3**, c) poly-**4**, d) poly-**5**, e) poly-**6**.

TGA studies

TGA traces were obtained in a TGA Q5000 (TA Instruments, New Castle, UK) using a platinum pan.

TGA Studies were carried out in order to determine the thermal stability of the polymers. As a general protocol, a polymer sample was kept in a platinum pan and heated from 40 °C to 800 °C with a heating rate if 10 °C/min (Figure S9).

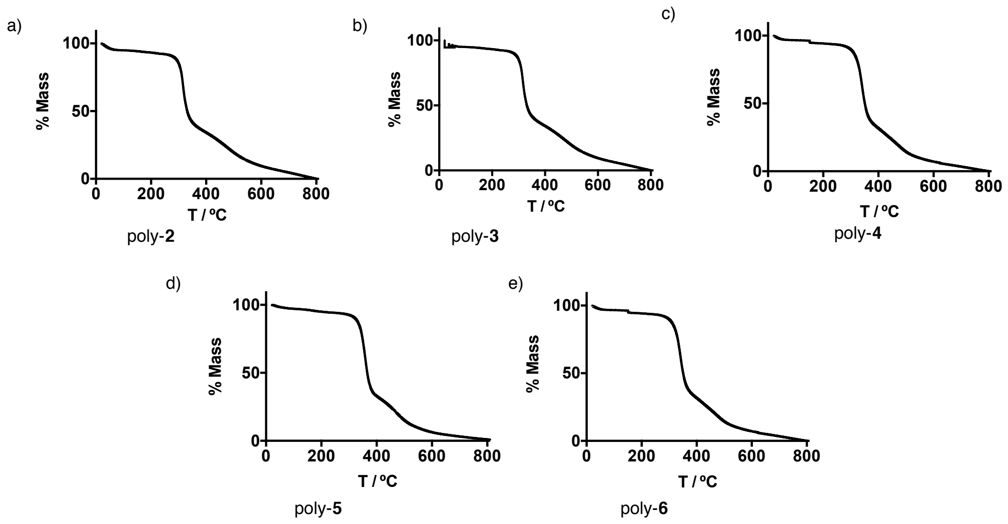

poly-**2** poly-**3** poly-**4** poly-**5** poly-**6**

Figure S9: TGA thermograms of a) poly-**2**, b) poly-**3**, c) poly-**4**, d) poly-**5**, e) poly-**6**.

3. IR measurements of different polymers

ATR/FT-IR spectra were recorded in a BRUKER IFS-66v spectrophotometer. A solution of $Ba(ClO_4)_2$ (0.2 equiv., 10.0 mg mL^{-1} in MeOH) was added to a solution of poly-**X** (X= poly-**2**, poly-**3**, poly-**4**, poly-**5**, poly-**6**) in $CHCl_3$ (1.5 mg mL^{-1}). The mixture was allowed to react for 5 minutes without stirring. FT-IR experiments show that, after the addition of $Ba(ClO_4)_2$ [poly-**X** / Ba^{2+} / MeOH in a 1.0/0.2/<500 mole ratio] produce a helical inversion due to a chelation between the divalent metal ion and the amide and ester groups of the pendant moiety (Figures S10-S14). This helix inversion is due to a conformational change at the pendant moiety from a preferred *anti* conformation between the two carbonyl groups, towards a *syn* orientation, which stabilized by the divalent metal ion. Consecutive additions of methanol [poly-**X** / Ba^{2+} / MeOH in a 1.0/0.2/>500 mole ratio] produce another helical inversion, and the initial CD signature is recovered. At this point, the metal ion is still present, being coordinated only to the ester group (Figures S10-S14), stabilizing again the preferred *anti* conformation.

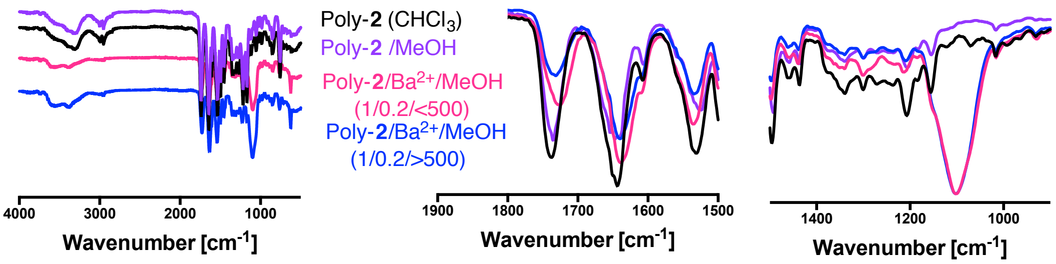

polymer	υ **CO$_1$**	υ **CO$_1$**	υ **OMe**	$\Delta\upsilon$ **CO$_1$**	$\Delta\upsilon$ **CO$_2$**	$\Delta\upsilon$ **OMe**
Poly-**2** **(**CHCl$_3$)	1643	1738	1053	-	-	-
Poly-**2** **(**CHCl$_3$)/MeOH	1643	1738	1053	-	-	-
Poly-**2**/Ba^{2+}/MeOH **(1/0.2/<500)**	1632	1728	1095	11	10	42
Poly-**2**/Ba^{2+}/MeOH **(1/0.2/>500)**	16336	1728	1099	7	10	46

Figure S10: IR spectra of solutions of poly-**2** in CHCl$_3$ (1.5 mg mL^{-1}) and solutions of polymers (1.5 mg mL^{-1} in CHCl$_3$) titrated with Ba(ClO$_4$)$_2$ in MeOH (10.0 mg mL^{-1}, 0.2 equiv.) and measured with both polymer(mru)/MeOH mole ratio= 1/<500 and polymer(mru)/MeOH mole ratio= 1/>500.

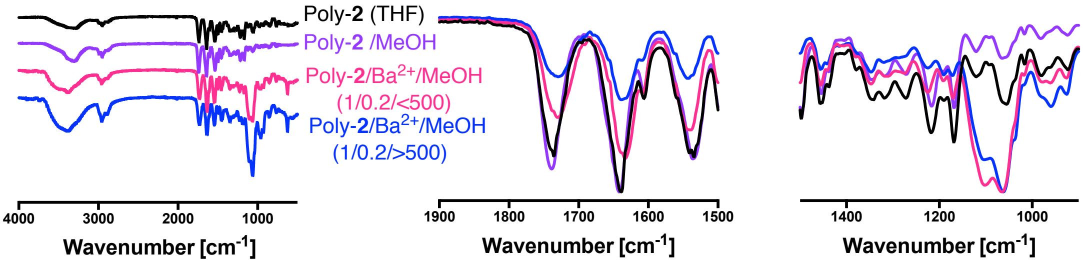

polymer	υ **CO$_1$**	υ **CO$_2$**	υ **OMe**	$\Delta\upsilon$ **CO$_1$**	$\Delta\upsilon$ **CO$_2$**	$\Delta\upsilon$ **OMe**
Poly-**2** (THF)	1639	1738	1053	-	-	-
Poly-**2** /MeOH	1639	1738	1053	0	0	0
Poly-**2**/Ba^{2+}/MeOH (1/0.2/<500)	1634	1733	1043	5	5	10
Poly-**2**/Ba^{2+}/MeOH (1/0.2/>500)	1639	1736	1041	0	2	12

Figure S11: IR spectra of solutions of poly-**2** in THF (1.5 mg mL^{-1}) and solutions of polymers (1.5 mg mL^{-1} in CHCl$_3$) titrated MeOH and with Ba(ClO$_4$)$_2$ in MeOH (10.0 mg mL^{-1}, 0.2 equiv.) and measured with both polymer(mru)/MeOH mole ratio= 1/<500 and polymer(mru)/MeOH mole ratio= 1/>500.

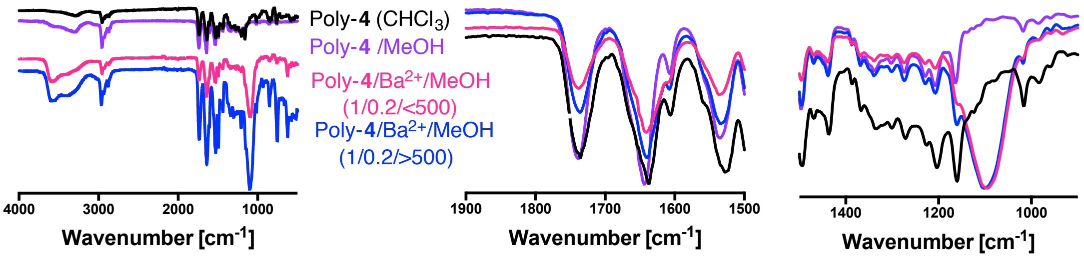

polymer	υ CO$_1$	υ CO$_2$	υ OMe	Δυ CO$_1$	Δυ CO$_2$	Δυ OMe
Poly-**4** ($CHCl_3$)	1637	1735	1016			
Poly-**4** ($CHCl_3$)/MeOH	1637	1735	1016	0	0	0
Poly-**4**/Ba^{2+}/MeOH (1/0.2/<500)	1641	1738	1097	4	3	81
Poly-**4**/Ba^{2+}/MeOH (1/0.2/>500)	1636	1729	1099	3	9	46

Figure S12: IR spectra of solutions of poly-**4** in $CHCl_3$ (1.5 mg mL^{-1}) and solutions of polymers (1.5 mg mL^{-1} in $CHCl_3$) titrated with MeOH and with $Ba(ClO_4)_2$ in MeOH (10.0 mg mL^{-1}, 0.2 equiv.) and measured with both polymer(mru)/MeOH mole ratio= 1/<500 and polymer(mru)/MeOH mole ratio= 1/>500.

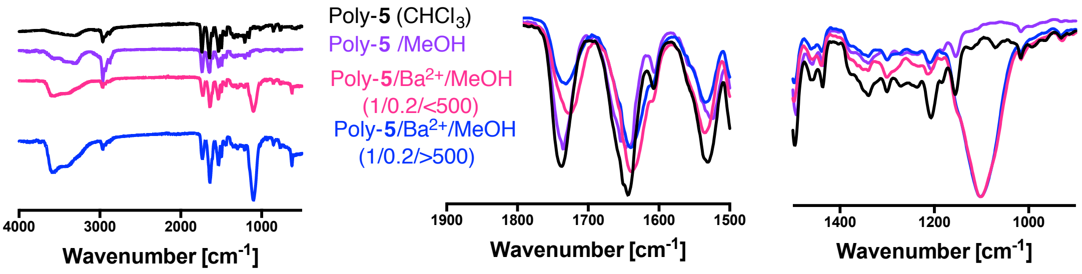

polymer	υ CO$_1$	υ CO$_2$	υ OMe	Δυ CO$_1$	Δυ CO$_2$	Δυ OMe
Poly-**5** ($CHCl_3$)	1640	1736	1080			
Poly-**5** ($CHCl_3$)/MeOH	1640	1736	1080	0	0	0
Poly-**5** /Ba^{2+}/MeOH (1/2.0/<300)	1628	1726	1121	12	10	41
Poly-**5** /Ba^{2+}/MeOH (1/2.0/>300)	1664	1725	1124	6	9	44

Figure S13: IR spectra of solutions of poly-**5** in $CHCl_3$ (1.5 mg mL^{-1}) and solutions of polymers (1.5 mg mL^{-1} in $CHCl_3$) titrated MeOH and with $Ba(ClO_4)_2$ in MeOH (10.0 mg mL^{-1}, 0.2 equiv.) and measured with both polymer(mru)/MeOH mole ratio= 1/<300 and polymer(mru)/MeOH mole ratio= 1/>300.

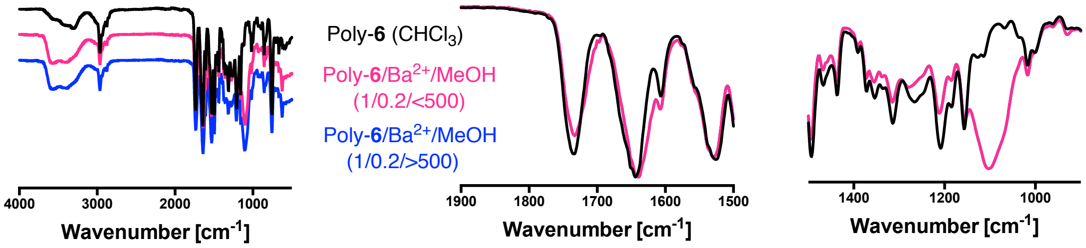

polymer	υ CO_1	υ CO_2	υ OMe	Δυ CO_1	Δυ CO_2	Δυ OMe
Poly-**6** ($CHCl_3$)	1643	1734	1016			
Poly-**6** /Ba^{2+}/MeOH (1/2.0/<300)	1639	1730	1032	4	4	16
Poly-**6** /Ba^{2+}/MeOH (1/2.0/>300)	1641	1730	1036	4	4	16

Figure S14: IR spectra of solutions of poly-**6** in $CHCl_3$ (1.5 mg mL^{-1}) and solutions of polymers (1.5 mg mL^{-1} in $CHCl_3$) titrated with $Ba(ClO_4)_2$ in MeOH (10.0 mg mL^{-1}, 0.2 equiv.) and measured with both polymer(mru)/MeOH mole ratio= 1/<300 and polymer(mru)/MeOH mole ratio= 1/>300.

4. CD studies

CD measurements were done in a Jasco-720. The amount of polymer used for CD measurements was 0.3 mg mL^{-1}.

4.1 Response of the polymers to external stimuli: solvents

The different responses of poly-**2**, poly-**3**, poly-**4**, poly-**5**, poly-**6** to a range of external stimuli such as solvents with different donor/acceptor/polarity characteristics were tested (Figure S15).

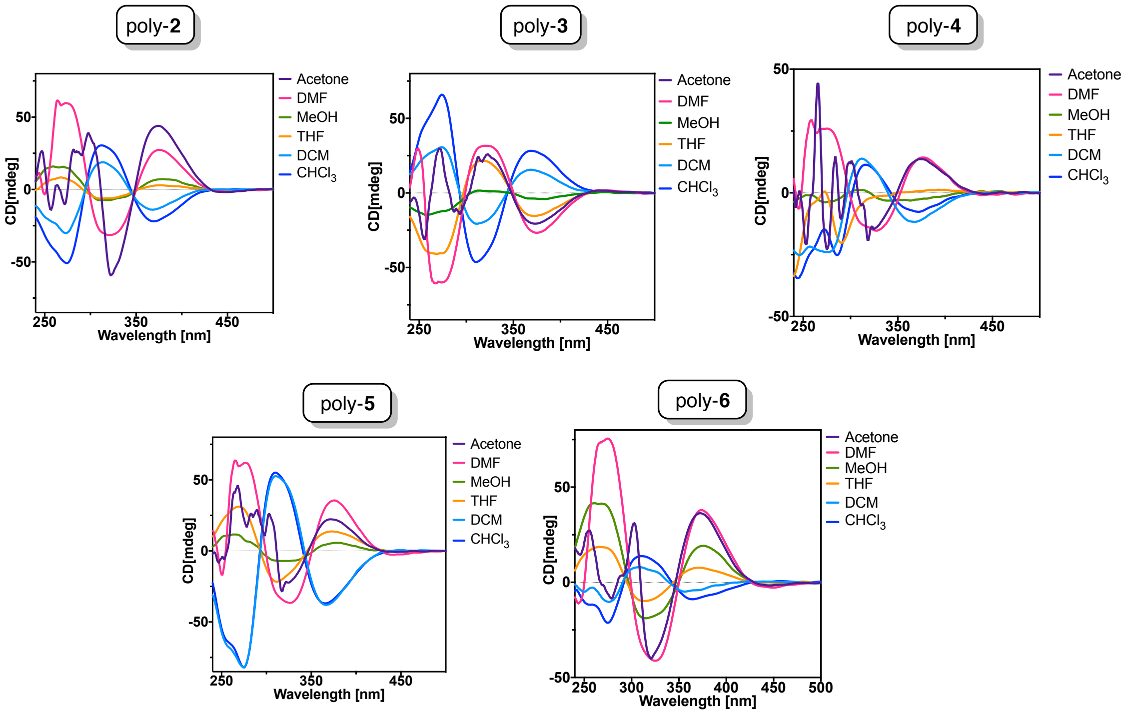

Figure S15: CD spectra of poly-**2**, poly-**3**, poly-**4** , poly-**5** and poly-**6** in different solvents.

4.2 Response of the polymers to external stimuli: metal cations

CD measurements were done in a Jasco-720. The amount of polymer used for CD measurements was 0.3 mg mL^{-1}.

CD studies were performed with a solution of poly-**2** in $CHCl_3$ (0.3 mg mL^{-1}) using different divalent metal ions of $M(ClO_4)_2$ in MeOH ($M^{2+}= Ca^{2+}$, Co^{2+}, Mg^{2+}, Mn^{2+}, Ni^{2+}, Pb^{2+}, Zn^{2+}, Fe^{2+}, Cu^{2+}) which concentration was 10.0 mg mL^{-1}.

Thus, at a poly-**2**(mru)/MeOH mole ratio= 1/<500, the CD spectra show a positive Cotton effect at the vinylic region indicating that the coordination of M^{2+} to the pendant is only through the carbonyl group. The helical polymer-metal complex adopts the *syn* conformation and, as a consequence, the left-handed helical structure (Figure S16). Further additions of methanol to that solution [poly-**2** / M^{2+} / MeOH in a 1.0/0.2/>500 mole ratio] produce another helical inversion leading now to the recovery of the initial CD signature (Figure S16).

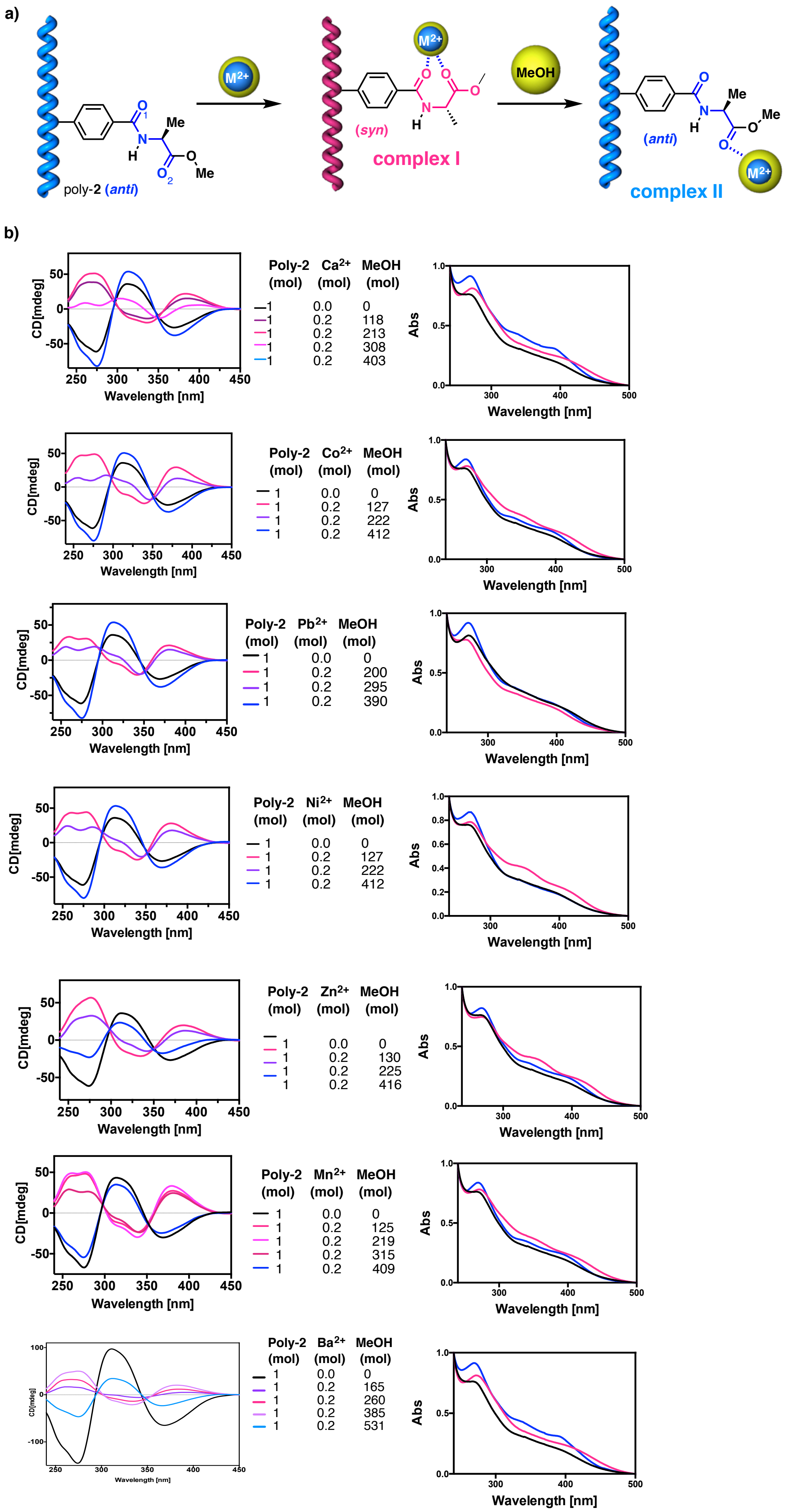
a)
M2+
MeOH
poly-2 (anti)
Me
N
H
O
1
O
2
O
Me
(syn)
complex I
(anti)
complex II
b)
CD[mdeg]
Wavelength [nm]
Abs
Poly-2 (mol) Ca2+ (mol) MeOH (mol)
1 0.0 0
1 0.2 118
1 0.2 213
1 0.2 308
1 0.2 403
Poly-2 (mol) Co2+ (mol) MeOH (mol)
1 0.0 0
1 0.2 127
1 0.2 222
1 0.2 412
Poly-2 (mol) Pb2+ (mol) MeOH (mol)
1 0.0 0
1 0.2 200
1 0.2 295
1 0.2 390
Poly-2 (mol) Ni2+ (mol) MeOH (mol)
1 0.0 0
1 0.2 127
1 0.2 222
1 0.2 412
Poly-2 (mol) Zn2+ (mol) MeOH (mol)
1 0.0 0
1 0.2 130
1 0.2 225
1 0.2 416
Poly-2 (mol) Mn2+ (mol) MeOH (mol)
1 0.0 0
1 0.2 125
1 0.2 219
1 0.2 315
1 0.2 409
Poly-2 (mol) Ba2+ (mol) MeOH (mol)
1 0.0 0
1 0.2 165
1 0.2 260
1 0.2 385
1 0.2 531
50
0
-50
100
-100
250
300
350
400
450
500
0.0
0.2
0.4
0.5
0.6
0.8
1.0

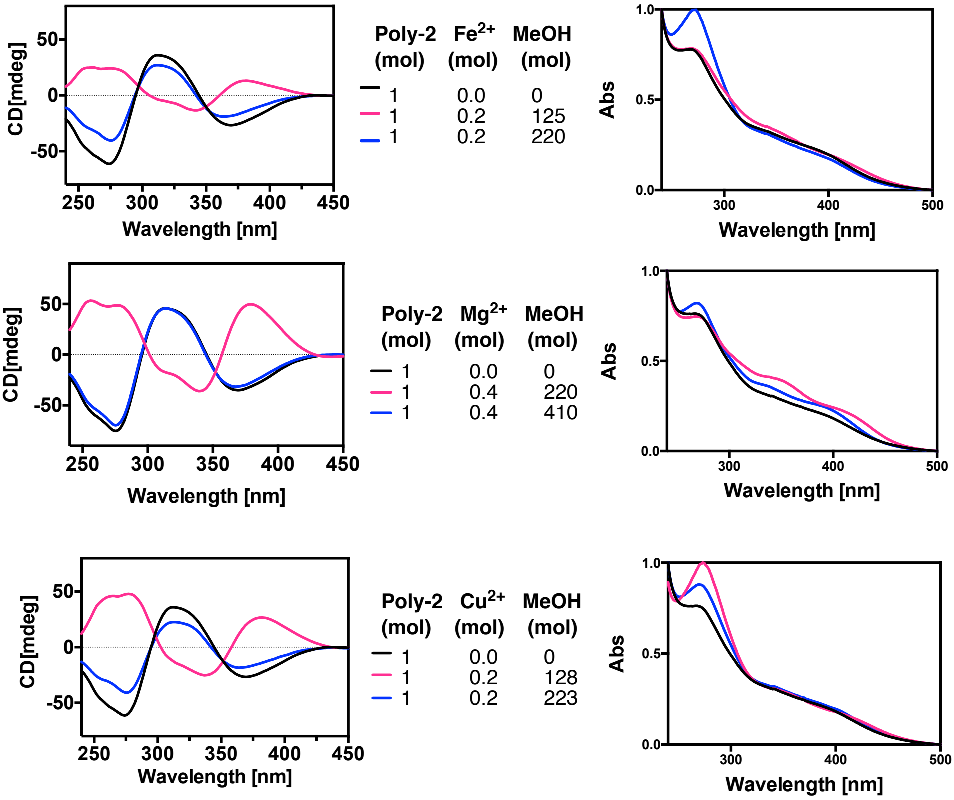

Figure S16: CD and UV spectra of a solution of poly-**2** (0.3 mg mL^{-1}) titrated with different divalent metal ions [$M(ClO_4)_2$ in MeOH] showing the dynamic metal coordination depending on the polymer/MeOH ratio.

Table S2: Limiting MeOH equivalents to obtain the Poly-**2** ($CHCl_3$)/M^{2+}/MeOH complex in its complex I or complex II form.

Poly-2/M^{2+} **(mol/mol)**	**Left handed helical sense** **(mol MeOH)**	**Right handed helical sense** **(mol MeOH)**
	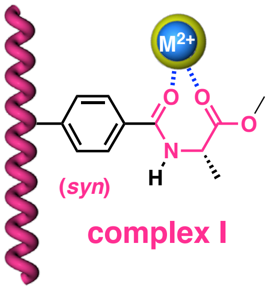	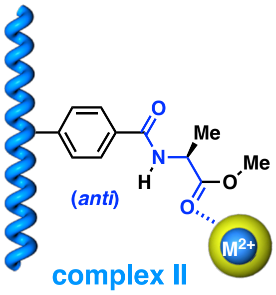
Poly-**2** ($CHCl_3$)/Ca^{2+} (1/0.2)	< 400	> 400
Poly-**2** ($CHCl_3$)/Co^{2+} (1/0.2)	< 400	> 400
Poly-**2** ($CHCl_3$)/Pb^{2+} (1/0.2)	< 400	> 400
Poly-**2** ($CHCl_3$)/Ni^{2+} (1/0.2)	< 400	> 400
Poly-**2** ($CHCl_3$)/Zn^{2+} (1/0.2)	< 400	> 400
Poly-**2** ($CHCl_3$)/Mn^{2+} (1/0.2)	< 400	> 400
Poly-**2** ($CHCl_3$)/Mg^{2+} (1/0.2)	< 400	> 400
Poly-**2** ($CHCl_3$)/Fe^{2+} (1/0.2)	< 220	> 220
Poly-**2** ($CHCl_3$)/Cu^{2+} (1/0.2)	< 220	> 220

Similar complexation experiments were performed for poly-**3,** poly-**4** and poly-**5** showing the same dynamic coordination mechanism in all polymers tested, with a first helix inversion due to the formation of complex I —chelation of the two carbonyls group (amide and ester) with the metal ion—, followed by a second helix inversion by addition of MeOH due to the formation of complex II –coordination of the metal to the ester group— (Figures S17, S18, S19).

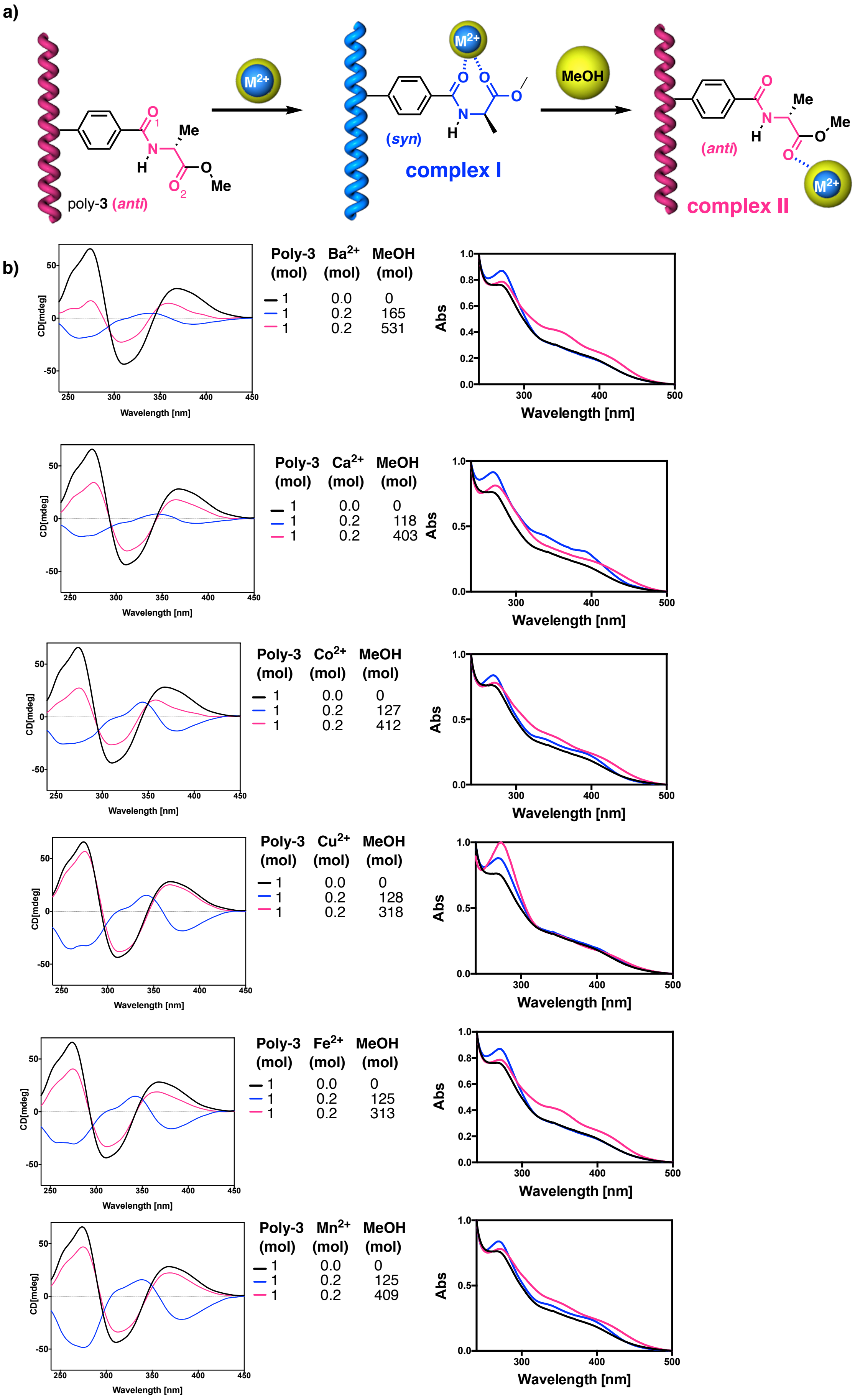
a)
M2+
MeOH
poly-3 (anti)
O 1
O 2
N
H
Me
O
Me
(syn)
complex I
(anti)
complex II
b)
CD[mdeg]
Wavelength [nm]
Abs
Wavelength [nm]
Poly-3 (mol) | Ba2+ (mol) | MeOH (mol)
1 | 0.0 | 0
1 | 0.2 | 165
1 | 0.2 | 531
Poly-3 (mol) | Ca2+ (mol) | MeOH (mol)
1 | 0.0 | 0
1 | 0.2 | 118
1 | 0.2 | 403
Poly-3 (mol) | Co2+ (mol) | MeOH (mol)
1 | 0.0 | 0
1 | 0.2 | 127
1 | 0.2 | 412
Poly-3 (mol) | Cu2+ (mol) | MeOH (mol)
1 | 0.0 | 0
1 | 0.2 | 128
1 | 0.2 | 318
Poly-3 (mol) | Fe2+ (mol) | MeOH (mol)
1 | 0.0 | 0
1 | 0.2 | 125
1 | 0.2 | 313
Poly-3 (mol) | Mn2+ (mol) | MeOH (mol)
1 | 0.0 | 0
1 | 0.2 | 125
1 | 0.2 | 409
50
0
-50
250
300
350
400
450
0.0
0.2
0.4
0.5
0.6
0.8
1.0
500

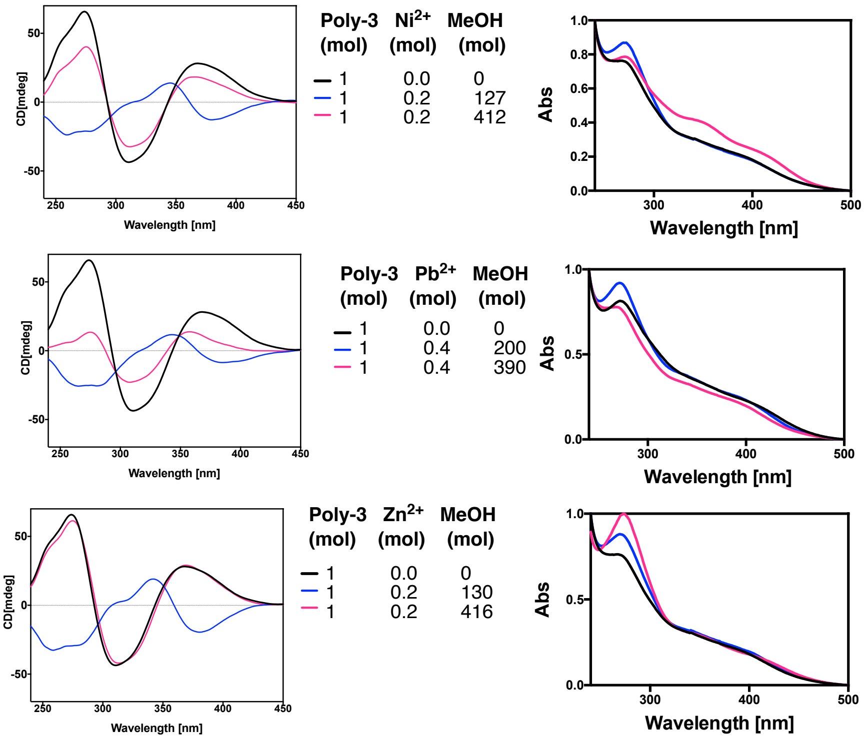

Figure S17: CD spectra of a solution of poly-**3** (0.3 mg mL^{-1}) titrated with different divalent metal ions [M(ClO$_4$)$_2$ in MeOH] showing the dynamic metal coordination depending on the polymer/MeOH ratio.

Table S3: Limiting MeOH equivalents to obtain the Poly-**3** (CHCl$_3$)/M^{2+}/MeOH complex in its complex I or complex II form.

Poly-3/M^{2+} **(mol/mol)**	**Right handed helical sense** **(mol MeOH)**	**Left handed helical sense** **(mol MeOH)**
	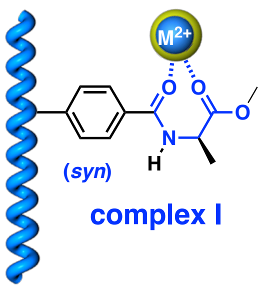	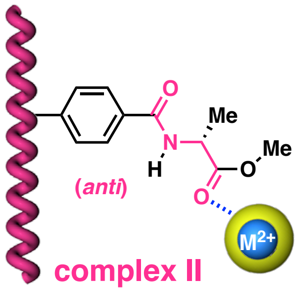
Poly-**3** (CHCl$_3$)/Ba^{2+} (1/0.2)	< 500	> 500
Poly-**3** (CHCl$_3$)/Ca^{2+} (1/0.2)	< 400	> 400
Poly-**3** (CHCl$_3$)/Co^{2+} (1/0.2)	< 400	> 400

Poly-**3** ($CHCl_3$)/Pb^{2+} (1/0.2)	< 400	> 400
Poly-**3** ($CHCl_3$)/Ni^{2+} (1/0.2)	< 400	> 400
Poly-**3** ($CHCl_3$)/Mn^{2+} (1/0.2)	< 400	> 400
Poly-**3** ($CHCl_3$)/Fe^{2+} (1/0.2)	< 300	> 300
Poly-**3** ($CHCl_3$)/Cu^{2+} (1/0.2)	< 300	> 300

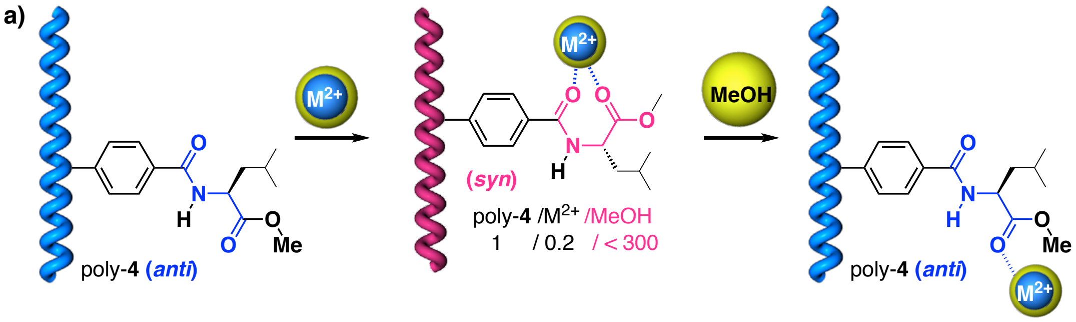
a)
M^{2+}
poly-4 (anti)
(syn)
poly-4 /M^{2+} /MeOH
1 / 0.2 / < 300
MeOH
poly-4 (anti)
O
N
H
O
Me
M^{2+}

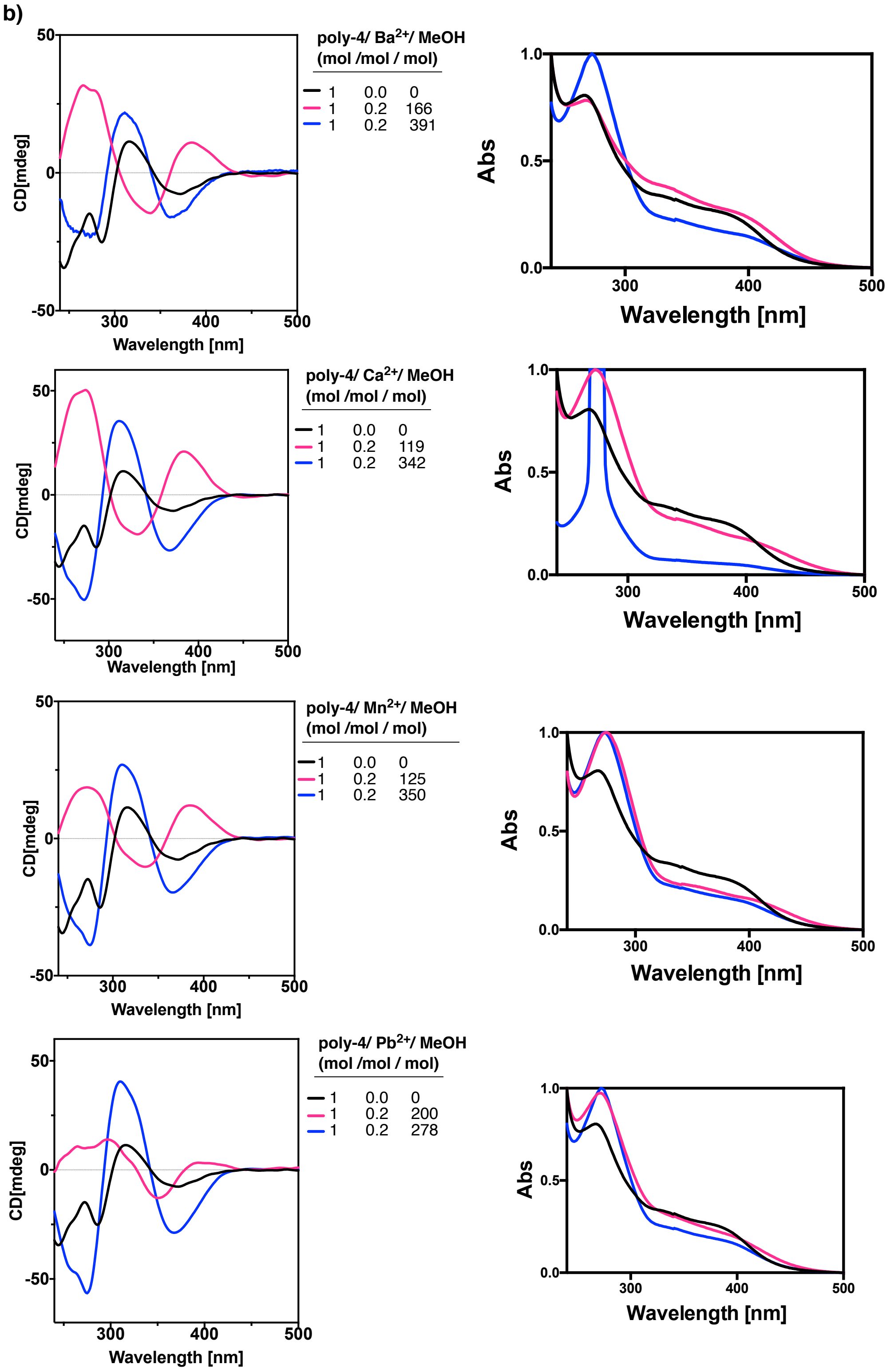
b)
poly-4/ Ba^{2+}/ MeOH
(mol /mol / mol)
1 0.0 0
1 0.2 166
1 0.2 391
poly-4/ Ca^{2+}/ MeOH
(mol /mol / mol)
1 0.0 0
1 0.2 119
1 0.2 342
poly-4/ Mn^{2+}/ MeOH
(mol /mol / mol)
1 0.0 0
1 0.2 125
1 0.2 350
poly-4/ Pb^{2+}/ MeOH
(mol /mol / mol)
1 0.0 0
1 0.2 200
1 0.2 278
CD[mdeg]
50
0
-50
300
400
500
Wavelength [nm]
Abs
1.0
0.5
0.0

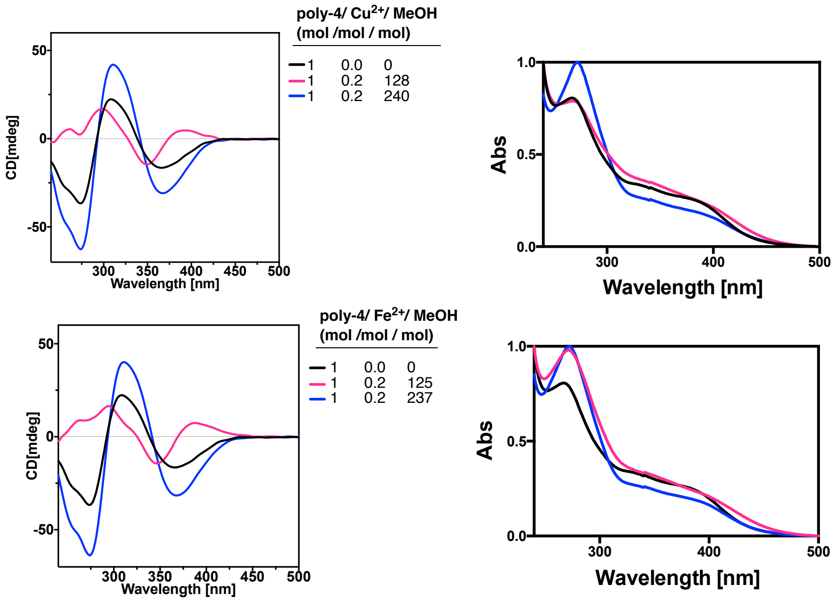

Figure S18: CD and UV spectra of a solution of poly-**4** (0.3 mg mL^{-1}) titrated with different divalent metal ions [M(ClO$_4$)$_2$ in MeOH] showing the dynamic metal coordination depending on the polymer/MeOH ratio.

Table S4: Limiting MeOH equivalents to obtain the Poly-**4** (CHCl$_3$)/M^{2+}/MeOH complex in its complex I or complex II form.

Poly-4/M^{2+} (mol/mol)	**Left handed helical sense (mol MeOH)**	**Right handed helical sense (mol MeOH)**
	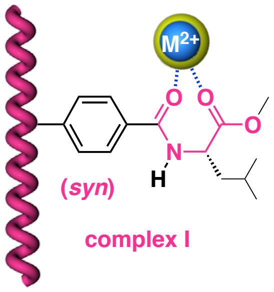	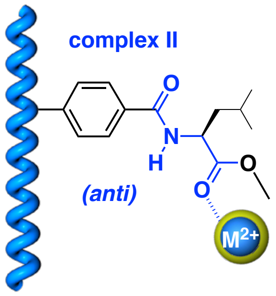
Poly-**4** (CHCl$_3$)/Ba^{2+} (1/0.2)	< 500	> 500
Poly-**4** (CHCl$_3$)/Ca^{2+} (1/0.2)	< 400	> 400
Poly-**4** (CHCl$_3$)/Zn^{2+} (1/0.2)	< 400	>400
Poly-**4**(CHCl$_3$)/Mn^{2+} (1/0.2)	< 350	> 350
Poly-**4** (CHCl$_3$)/Pb^{2+} (1/0.2)	< 270	> 270

Poly-**4** (CHCl$_3$)/Fe^{2+} (1/0.2)	< 240	> 240
Poly-**4** (CHCl$_3$)/Zn^{2+} (1/0.2)	< 240	> 240

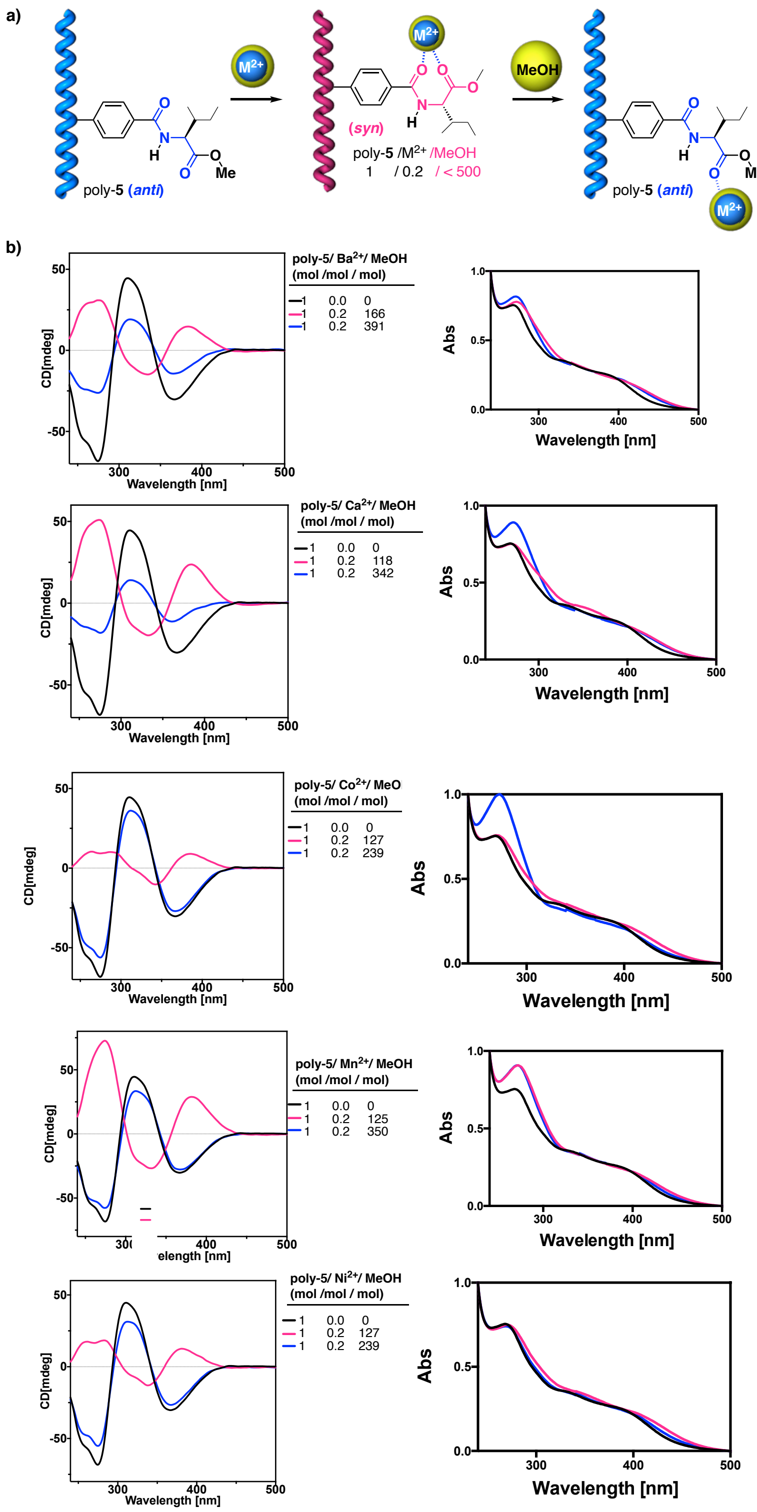

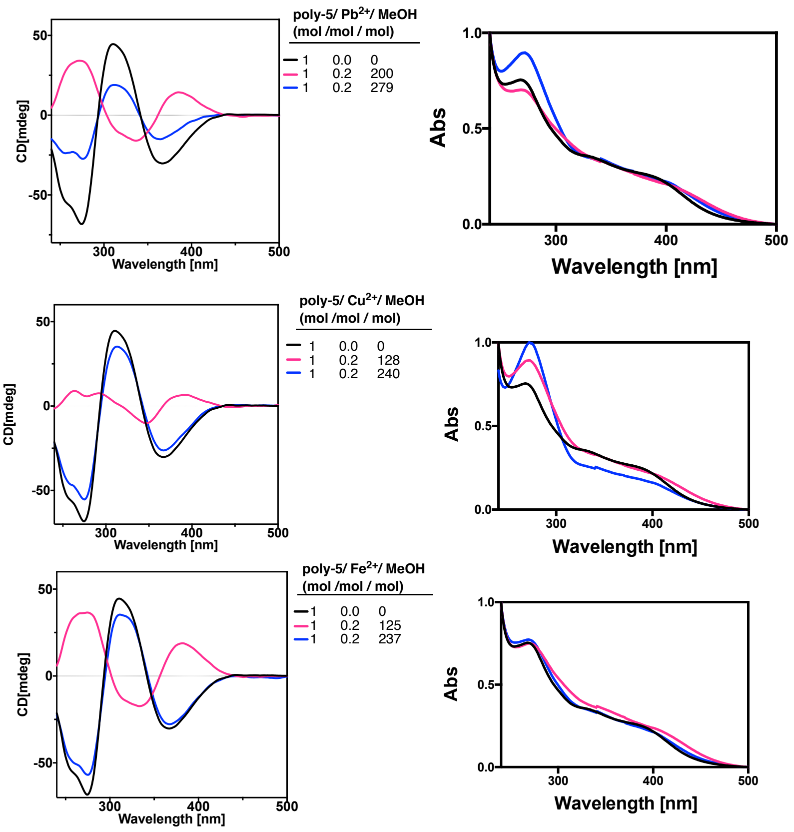

Figure S19: CD and UV spectra of a solution of poly-**5** (0.3 mg mL^{-1}) titrated with different divalent metal ions [$M(ClO_4)_2$ in MeOH] showing the dynamic metal coordination depending on the polymer/MeOH ratio.

Table S5: Limiting MeOH equivalents to obtain the Poly-**5** ($CHCl_3$)/M^{2+}/MeOH complex in its complex I or complex II form.

Poly-5/M^{2+} **(mol/mol)**	**Left handed helical sense** **(mol MeOH)**	**Right handed helical sense** **(mol MeOH)**
	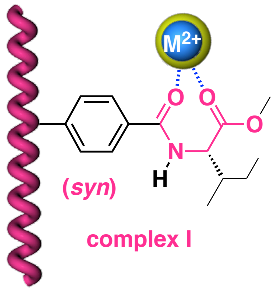	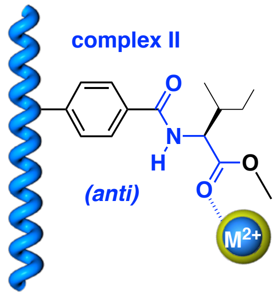
Poly-**5** ($CHCl_3$)/Ba^{2+} (1/0.2)	< 400	> 400
Poly-**5** ($CHCl_3$)/Mn^{2+} (1/0.2)	< 350	> 350
Poly-**5** ($CHCl_3$)/Ca^{2+} (1/0.2)	< 320	> 320

Poly-**5** (CHCl$_3$)/Cu^{2+} (1/0.2)	< 240	> 240
Poly-**5** (CHCl$_3$)/Ni^{2+} (1/0.2)	< 240	> 240
Poly-**5** (CHCl$_3$)/Co^{2+} (1/0.2)	< 240	> 240
Poly-**5** (CHCl$_3$)/Fe^{2+} (1/0.2)	< 240	> 240
Poly-**5** (CHCl$_3$)/Pb^{2+} (1/0.2)	< 280	> 280

In the case poly-**6** (CHCl$_3$), there is an exception for the second helix inversion: although the complex II is obtained —metal coordinated only to the ester group—, the conformation at the pendant group remains *syn*, without recovering the initial *anti* conformation.

Additional studies on the dynamic behaviour of poly-**6** in CHCl$_3$ showed that the addition of tiny amounts of MeOH stabilizes the *syn* conformation at the pendant moiety, making impossible to recover the original *anti* conformation adopted by poly-**6** in CHCl$_3$ (Figure S20).

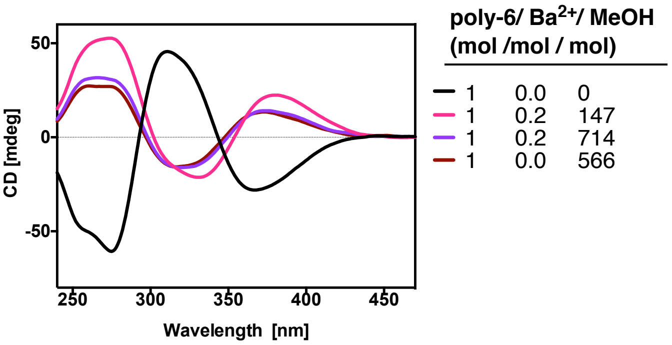

Figure S20: CD spectra of poly-**6** with different metal ions showing the dynamic metal coordination depending on the polymer/MeOH ratio.

Studies with monovalent metal ions:

Similar complexation studies were performed with a solution of the different polymers in CHCl$_3$ (0.3 mg mL^{-1}) using, in this case, different monovalent metal ions of MClO$_4$ in MeOH (M$^+$= Li$^+$, Ag$^+$; 10.0 mg mL^{-1}). The helical induction by the metal ion (complex I) and the subsequent inversion by the cosolvent (complex II) was also observed, showing the same dynamic coordination mechanism as with divalent metal ions, proving the general character and robustness of this methodology (PPA-aa-OMe / Metal ion complex, Figure S21).

Helical switch via dynamic cordination chemistry: Monovalent metal ions

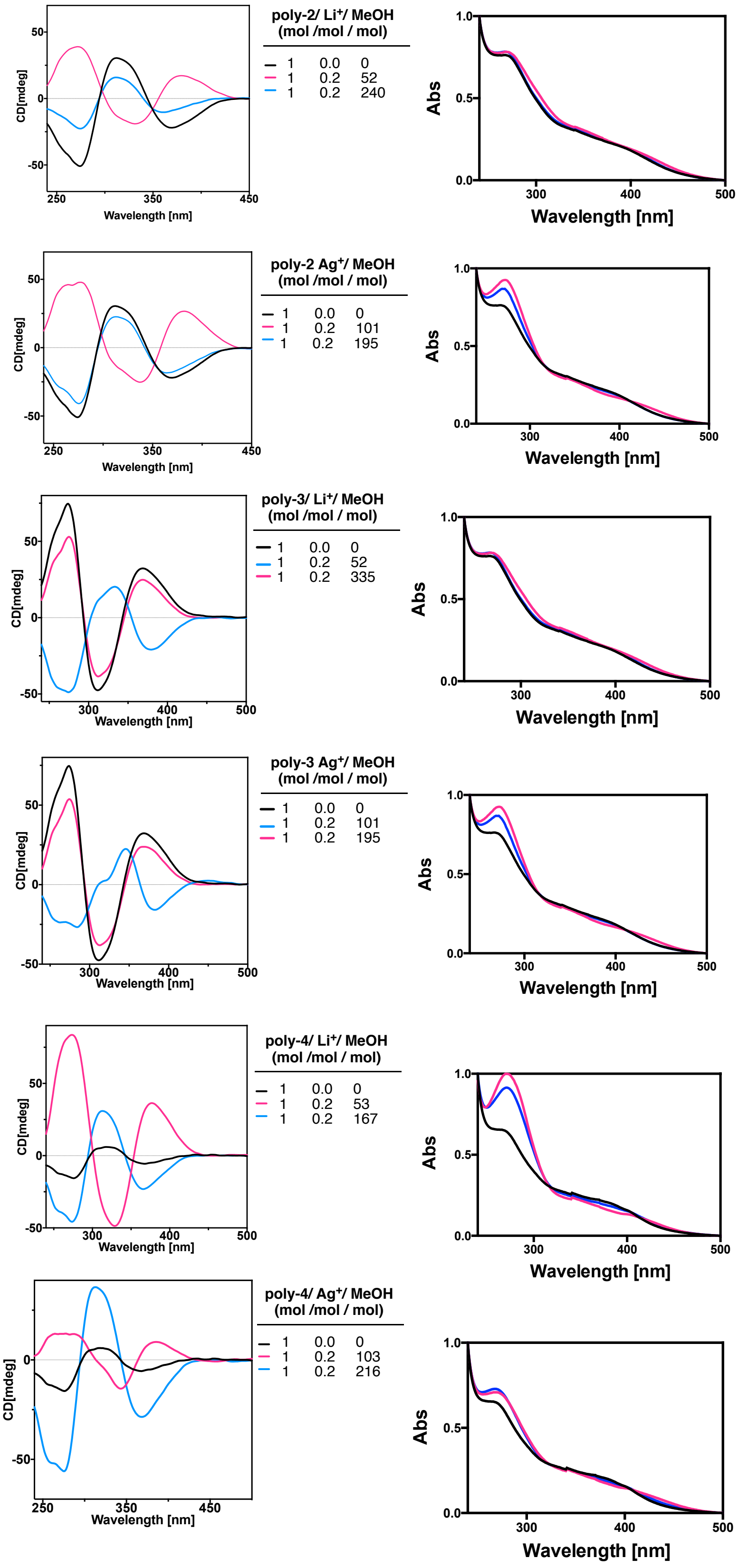

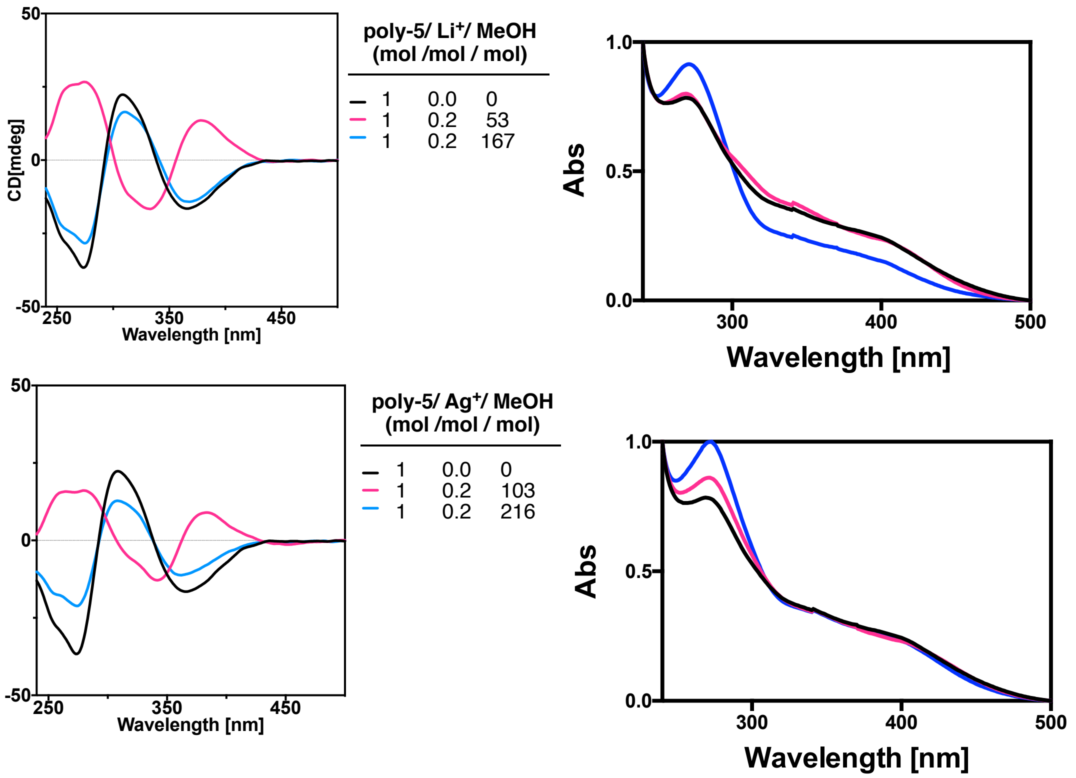

Figure S21: CD and UV spectra of 0.3 mg mL^{-1} of poly-**2**, poly-**3**, poly-**4**, poly-**5** in $CHCl_3$ with 10 mg mL^{-1} of monovalent metal ions (Li^+, Ag^+) dissolved in MeOH.

Table S6: Limiting MeOH equivalents to obtain the Poly-**(2-5)** ($CHCl_3$)/M^+/MeOH complex in its complex I or complex II form.

Poly-2 / M$^+$ (mol/mol)	**Left handed helical sense (mol MeOH)**	**Right handed helical sense (mol MeOH)**
	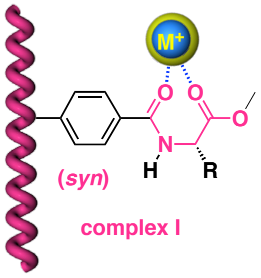	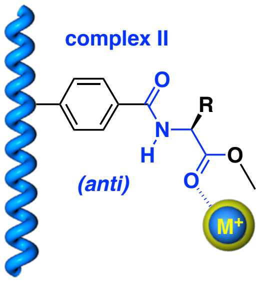
Poly-**2** ($CHCl_3$)/Li^{2+} (1/0.2)	< 240	> 240
Poly-**2** ($CHCl_3$)/Ag^+ (1/0.2)	< 200	> 200
Poly-**4** ($CHCl_3$)/Li^+ (1/0.2)	< 170	> 170

Poly-**4** ($CHCl_3$)/Ag^+ (1/0.2)	< 220	> 220
Poly-**5** ($CHCl_3$)/Li^+ (1/0.2)	< 170	> 170
Poly-**5** ($CHCl_3$)/Ag^+ (1/0.2)	< 220	> 220

Table S7: Limiting MeOH equivalents to obtain the Poly-(**3**) ($CHCl_3$)/M^+/MeOH complex in its complex I or complex II form.

Poly-2 / M^+ (mol/mol)	**Right handed helical sense (mol MeOH)**	**Left handed helical sense (mol MeOH)**
	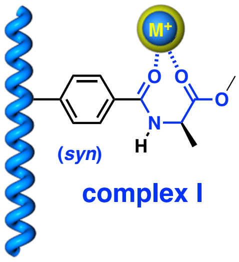	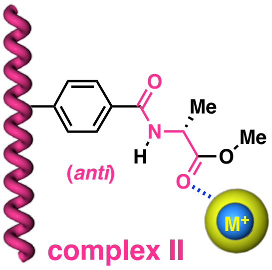
Poly-**3** ($CHCl_3$)/Li^+ (1/0.2)	> 300	< 300
Poly-**3**($CHCl_3$)/Ag^+ (1/0.2)	> 200	< 200

5. Nanostructuration studies

5.1 Dynamic light scattering (DLS) measurements

DLS measurements were performed on a Malvern Nano ZS (Malvern Instruments, U.K.) operating at 633 nm with a 173° scattering angle. Samples were measured at a final concentration of 0.3 mg mL^{-1} diluted with $CHCl_3$. These studies clearly indicate that HPMCs form aggregates with a defined structure.

The size of these aggregates can be modulated by the addition of different divalent metal ions or different amounts of the metal.

Addition of $M(ClO_4)_2$ to solutions of poly-**2** in $CHCl_3$ (0.3 mg mL^{-1}) at an appropriate poly-**2**(mru)/M^{2+} ratio originates the appearance of well defined nanospheres (i.e., a poly-**2**(mru)/Ba^{2+} ratio of 1.0/0.2 generate nanospheres of 75 nm; Figure S22).

Additional studies were carried out on solutions of poly-**2** in $CHCl_3$ (0.3 mg mL^{-1}) with the addition of $M(ClO_4)_2$ and with a poly-**2**(mru)/MeOH mole ratio= 1/>500. The formation of chiral nanoparticles was observed. DLS studies show larger chiral aggregates with a right-handed helix when the polymer/MeOH mole ratio= 1/>500 (Figure S22).

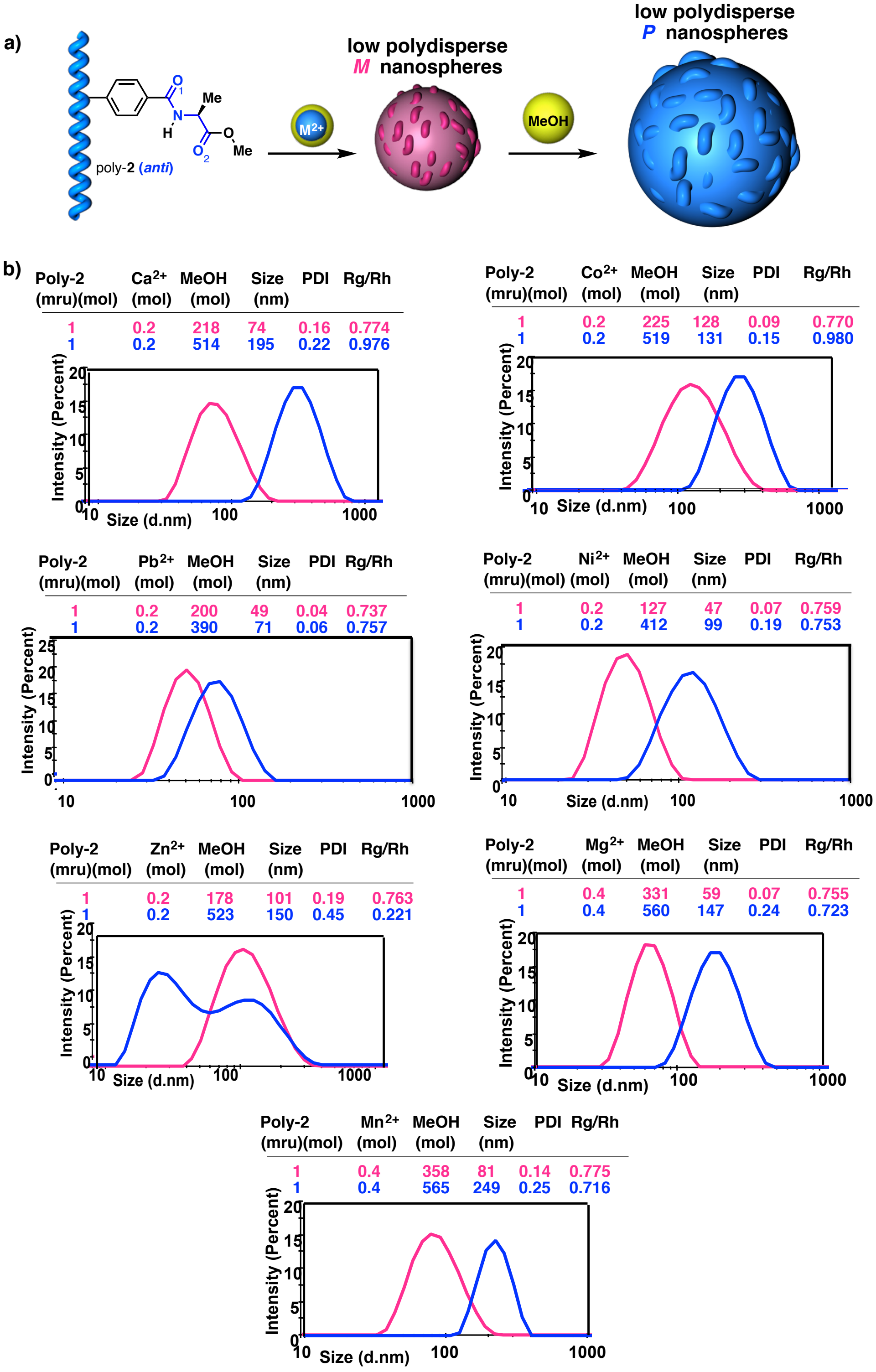

Poly-2 (mru)(mol)	Ca^{2+} (mol)	MeOH (mol)	Size (nm)	PDI	Rg/Rh
1	0.2	218	74	0.16	0.774
1	0.2	514	195	0.22	0.976

Poly-2 (mru)(mol)	Co^{2+} (mol)	MeOH (mol)	Size (nm)	PDI	Rg/Rh
1	0.2	225	128	0.09	0.770
1	0.2	519	131	0.15	0.980

Poly-2 (mru)(mol)	Pb^{2+} (mol)	MeOH (mol)	Size (nm)	PDI	Rg/Rh
1	0.2	200	49	0.04	0.737
1	0.2	390	71	0.06	0.757

Poly-2 (mru)(mol)	Ni^{2+} (mol)	MeOH (mol)	Size (nm)	PDI	Rg/Rh
1	0.2	127	47	0.07	0.759
1	0.2	412	99	0.19	0.753

Poly-2 (mru)(mol)	Zn^{2+} (mol)	MeOH (mol)	Size (nm)	PDI	Rg/Rh
1	0.2	178	101	0.19	0.763
1	0.2	523	150	0.45	0.221

Poly-2 (mru)(mol)	Mg^{2+} (mol)	MeOH (mol)	Size (nm)	PDI	Rg/Rh
1	0.4	331	59	0.07	0.755
1	0.4	560	147	0.24	0.723

Poly-2 (mru)(mol)	Mn^{2+} (mol)	MeOH (mol)	Size (nm)	PDI	Rg/Rh
1	0.4	358	81	0.14	0.775
1	0.4	565	249	0.25	0.716

Figure S22: DLS measurements for 0.3 mg mL^{-1} poly-**2** in $CHCl_3$ titrated different $M(ClO_4)_2$.

The robustness of this procedure to prepare chiral polymer particles was also tested with poly-**3** / M^{n+} / MeOH and poly-**4** / M^{n+} / MeOH (Figure S23, S24). For poly-**4**, consecutive additions of MeOH [poly-**4** / M^{2+} / MeOH in a 1.0/0.2/>300 mole ratio] produce another helical inversion, and the initial CD signature is recovered (similar to poly-**2**). However, the amount of methanol prevents the formation of well-defined *P* nanoparticle due to the solvation of the metal promoted by the co-solvent. Therefore, if we change MeOH by another donator co-solvent, such as THF, to decrease the solvation level, *P* nanoparticles can be obtained (Figure S24).

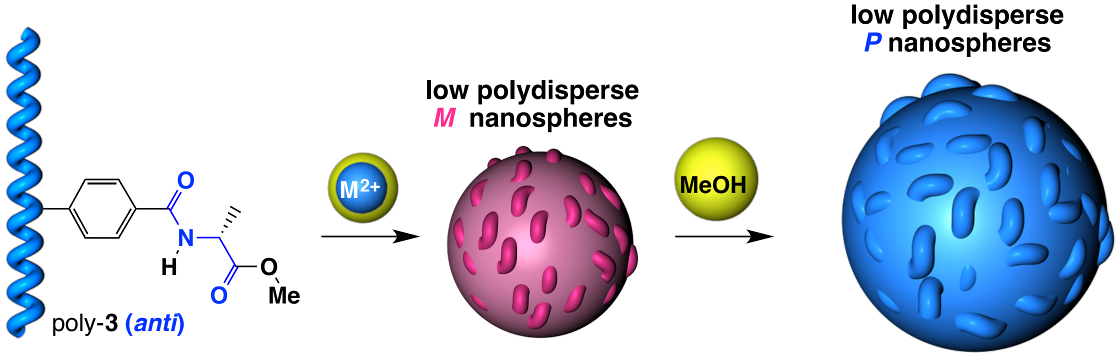

poly-3 (mru)(mol)	Ba^{2+} (mol)	MeOH (mol)	Size (nm)	PDI	Rg/Rh
1	0.0	0	34	0.245	0.400
1	0.2	165	71	0.063	0.722
1	0.2	531	97	0.145	0.981

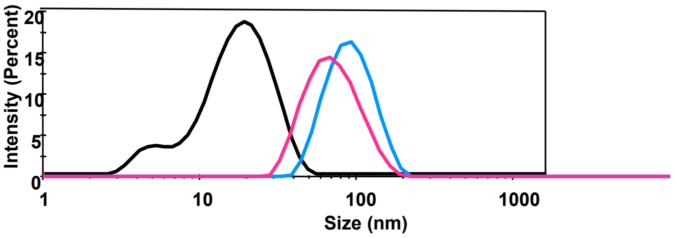

Figure S23: Conceptual representation and DLS measurements of the selective *P* or *M*-nanostructuration of the poly-**3**/Ba^{+} complex in $CHCl_3$ through dynamic coordination chemistry.

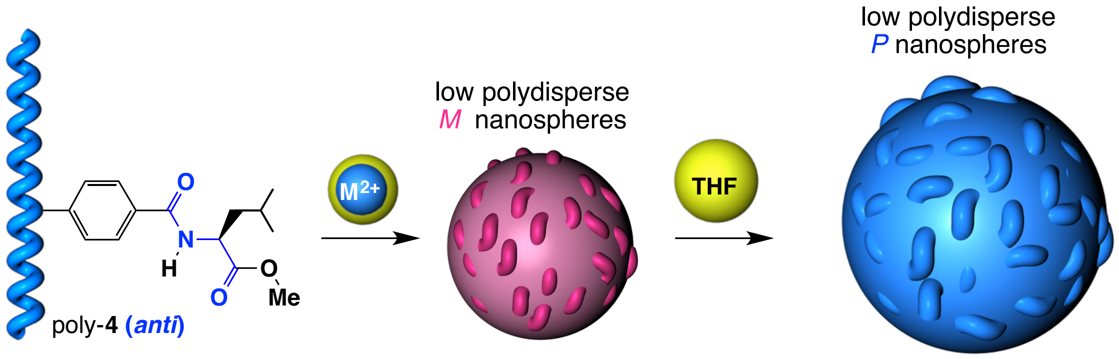

poly-4 (mru)(mol)	Ba^{2+} (mol)	MeOH (mol)	THF (mol)	Size (nm)	PDI	Rg/Rh
1	0.0	0	0	34	0.245	0.321
1	0.2	166	0	78	0.031	0.774
1	0.2	166	225	95	0.153	0.743

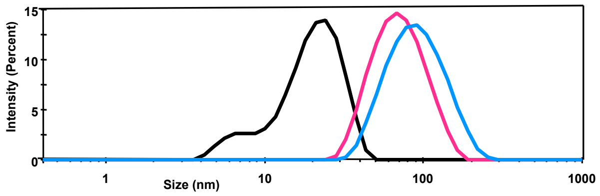

Figure S24: Conceptual representation and DLS measurements of the selective *P*- or *M*-nanostructuration of the poly-**4**/Ba^+ complex in $CHCl_3$ through dynamic coordination chemistry.

It was found that when beta branched amino acids are used as pendant groups in the poly-**5** (Figure S20a) and poly-**6** (Figure S20b) complex, the crosslinking ability of the metal is reduced or even disrupted due to the steric hindrance on the pendant group, and therefore chiral nanospheres are not obtained (Figure S25).

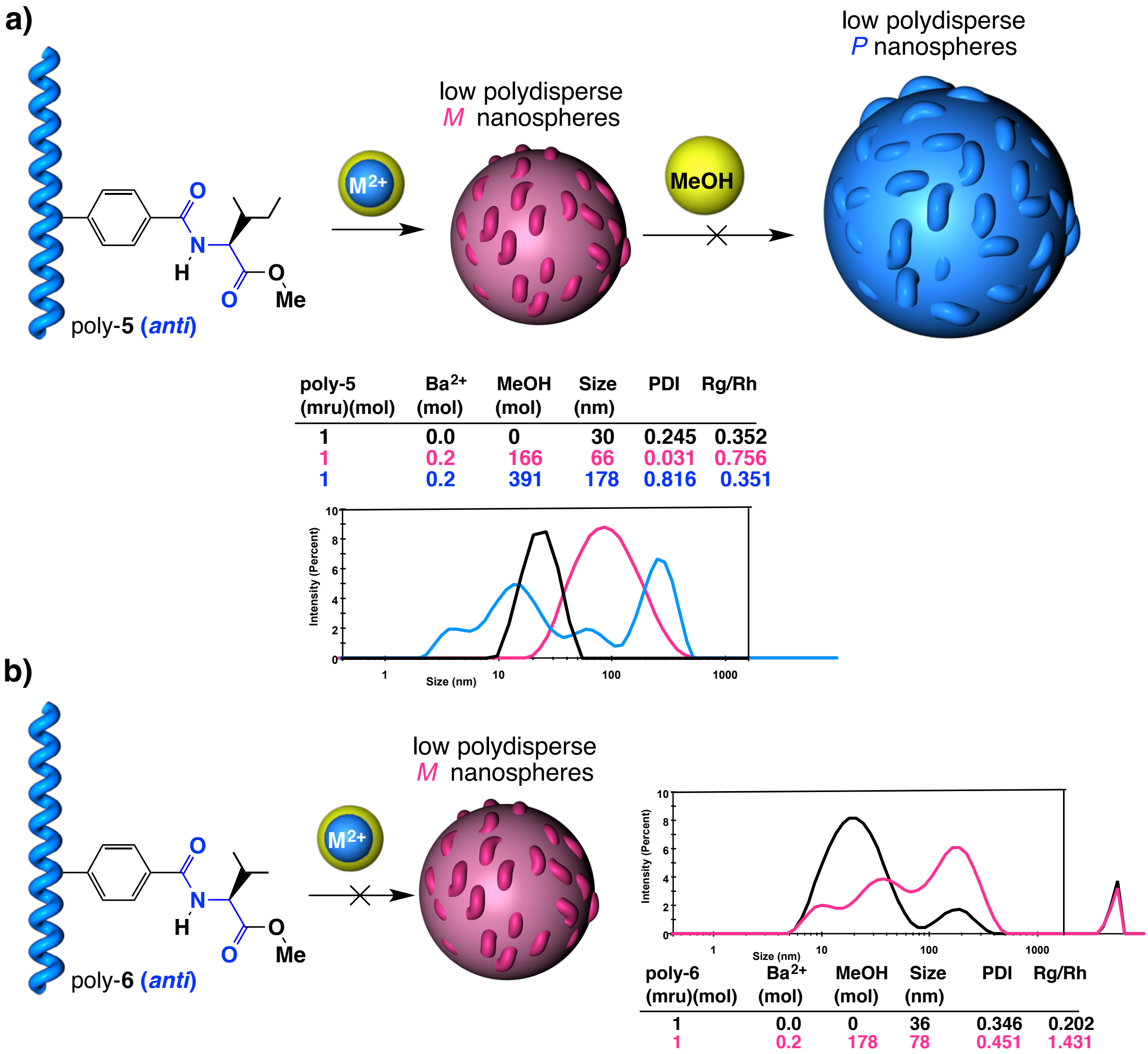

poly-5 (mru)(mol)	Ba^{2+} (mol)	MeOH (mol)	Size (nm)	PDI	Rg/Rh
1	0.0	0	30	0.245	0.352
1	0.2	166	66	0.031	0.756
1	0.2	391	178	0.816	0.351

poly-6 (mru)(mol)	Ba^{2+} (mol)	MeOH (mol)	Size (nm)	PDI	Rg/Rh
1	0.0	0	36	0.346	0.202
1	0.2	178	78	0.451	1.431

Figure S25: a) Conceptual representation and DLS measurements of the selective *M* nanostructuration of the poly-**5**/Ba^{+} complex in $CHCl_3$. b) Conceptual representation and DLS measurements showing that chiral nanospheres are not obtained for poly-**6**/Ba^{2+}.

5.2 Microscopy studies

SEM measurements were performed on a LEO-435VP electron microscope equipped with an energy dispersive X-ray (EDX) spectrometer.
TEM measurements were performed on a JEOL JEM 2010 and 200 KV as a voltage.

Measurements of left-handed HPMCs

A solution of poly-**2** in $CHCl_3$ (0.03 mg mL^{-1}) titrated with $M(ClO_4)_2$ (10.00 mg mL^{-1}, in MeOH) with poly-**2**(mru)/MeOH mole ratio=1/<500 showed a positive Cotton effect at the vinylic region in the CD spectra indicating the presence of a left-handed helical structure. This solution was drop casted onto a silicon wafer chip and allowed to dry at rt for 12 h, and SEM measurements were carried out.

For TEM measurements, a drop of a solution of poly-**2** (0.03 mg mL^{-1}) with different amounts of M(ClO_4)$_2$ was settled onto formvar carbon film, and allowed to dry at rt for 12 h.

During these measurements, the presence of nanospheres made of poly-**2**/M^{2+} complex was observed. In those nanospheres, the polymer adopts a preferred left-handed helical structure (Figure S26).

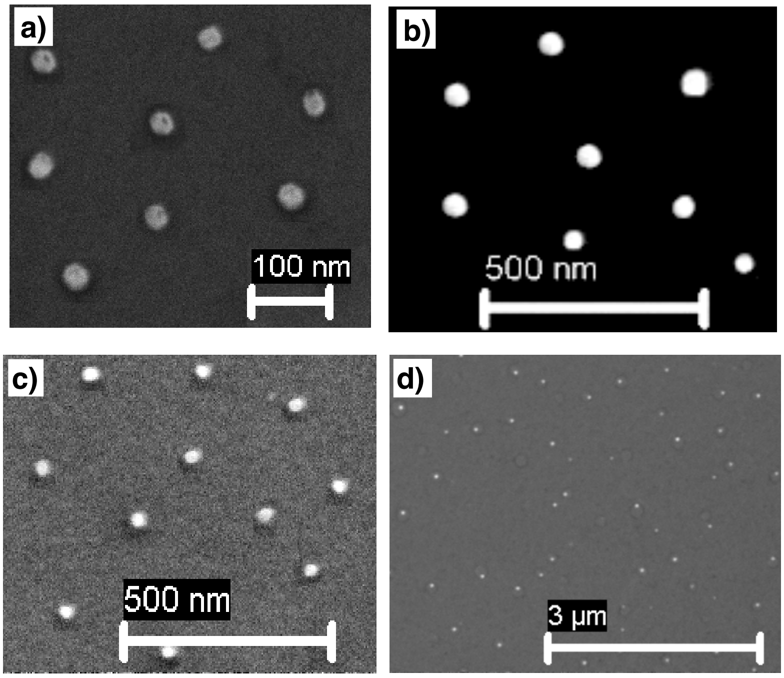

Figure S26: SEM images of left-handed nanospheres: a) 0.03 mg mL^{-1} of poly-**2** and 0.2 equiv. of Ba(ClO_4)$_2$ (MeOH) (diameter 38±3 nm, scale bar 100 nm, 8 particles), b) 0.03 mg mL^{-1} of poly-**2** and 0.2 equiv. of Ba(ClO_4)$_2$ (MeOH) (diameter 56±7 nm, scale bar 500 nm, 8 particles) and c) 0.03 mg mL^{-1} of poly-**2** and 0.2 equiv. of Ba(ClO_4)$_2$ (MeOH) (diameter 37±6 nm, scale bar 200 nm, 11 particles), d) 0.03 mg mL^{-1} of poly-**2** and 0.2 equiv. of Ba(ClO_4)$_2$ (MeOH) (diameter 52±11 nm, scale bar 3 μm 37 particles).

Measurements of right-handed HPMCs

A solution of poly-**2** in $CHCl_3$ (0.03 mg mL^{-1}) titrated with Ba(ClO_4)$_2$ (10.00 mg mL^{-1}) and poly-**2**(mru)/MeOH mole ratio=1/>500, showed a negative Cotton effect at the vinylic region indicating the initial CD signature is recovered. Moreover, the metal ion is still present being coordinated only to ester group stabilizing again the preferred *anti* conformation. This solution was drop casted onto a silicon wafer chip and allowed to dry at rt for 12 h, and SEM measurements were carried out. During these studies, the presence of *P*-

nanospheres with a size between 90 and 120 nm made from poly-**2**/Ba$^+$ complex were observed (Figure S22).

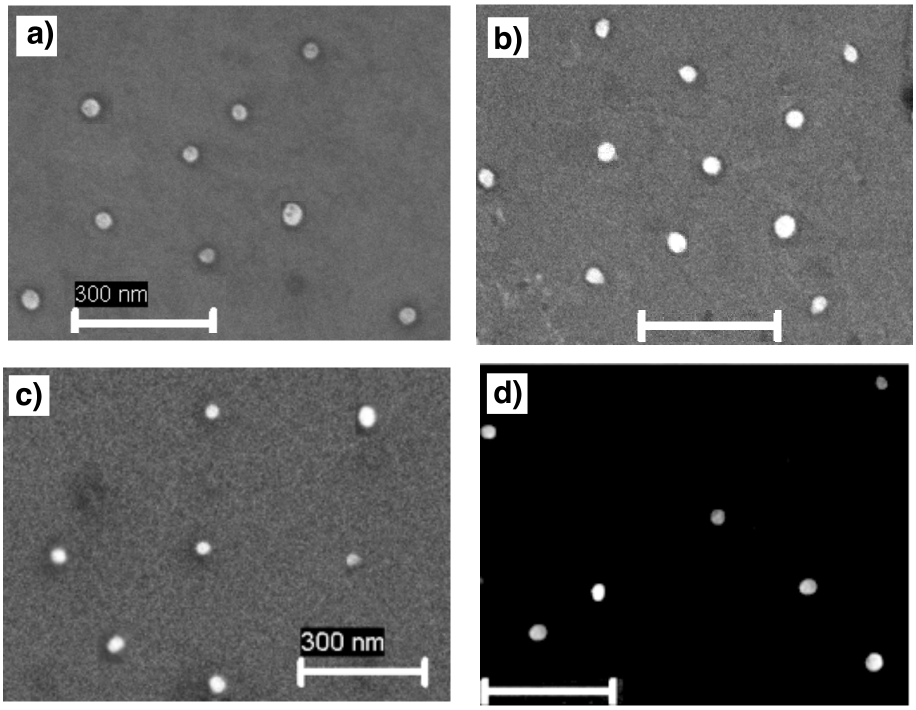

Figure S27: SEM images of right-handed nanospheres: a) 0.03 mg mL^{-1} of poly-**2** and 0.4 equiv. of Ba(ClO$_4$)$_2$ (MeOH) (diameter 34±4 nm, scale bar 300 nm, 9 particles), b) 0.03 mg mL^{-1} of poly-**2** and 0.2 equiv. of Ba(ClO$_4$)$_2$ (MeOH) (diameter 33±6 nm, scale bar 300 nm, 12 particles), c) 0.03 mg mL^{-1} of poly-**2** and 0.2 equiv. of Ba(ClO$_4$)$_2$ (MeOH) (diameter 41±16 nm, scale bar 300 nm, 7 particles), d) 0.03 mg mL^{-1} of poly-**2** and 0.2 equiv. of Ba(ClO$_4$)$_2$ (MeOH) (diameter 31±13 nm, scale bar 300 nm, 8 particles).

5.3 Encapsulation studies: confocal microscopy

Images were performed on a Leica TSC-SP2 microscope. Solutions of poly-**2** in CHCl$_3$ (0.03 mg mL^{-1}) with the correspondent fluorescent dyes (5,6-carboxyfluorescein, rhodamine B isothiocyanate) or Quantum Dots [Lumidot CdSe/ZnS (590 nm QD)] and different divalent metal ions M(ClO$_4$)$_2$ in MeOH (10 mg mL^{-1}) were carried out. The HPMC with poly-**2**(mru)/MeOH mole ratio=1/<500 and poly-**2**(mru)/MeOH mole ratio=1/>500 generates selectively chrial (*M* or *P*) nanoparticles (Figure S23).

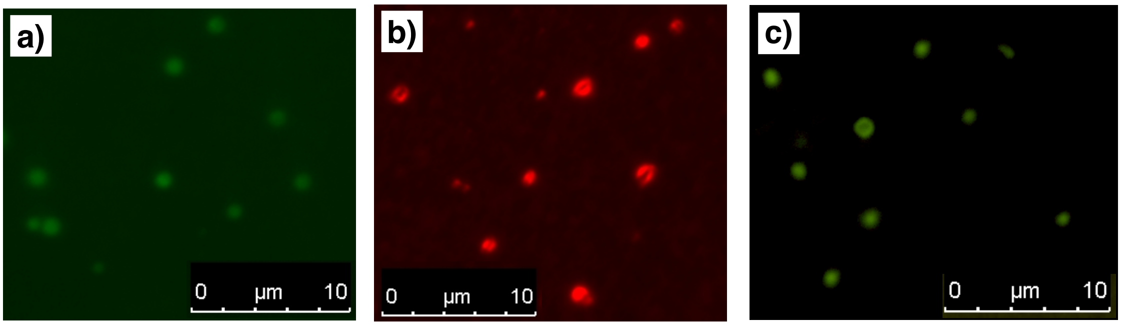

Figure S28: Confocal images of: a) *M* nanospheres containing 5,6-carboxyfluorescein, b) *M* nanospheres containing rhodamine B isothiocyanate, and c) *P* nanospheres containing quantum dots [Lumidot CdSe/ZnS (590nm QD)].

5.4 Atomic force microscopy (AFM) measurements

Stock solutions of poly-**2** (0.3 mg mL^{-1}) in $CHCl_3$ were prepared and then diluted until 0.03 mg/mL. A solution of 10 mg/mL of $Ba(ClO_4)_2$ in MeOH was prepared and 0.2 equiv. of Ba^{2+} were added to a 0.03 mg mL^{-1} solution of poly-**2** in $CHCl_3$. One drop of this mixture (10 μL) was placed on freshly cleaved onto silicon wafer chip (Figure S24).

All AFM measurements were performed at Park System in air at RT with standard silicon cantilevers and super-sharp cantilevers in non-contact mode using 12 μm and 1 μm scanners.

Nanoscope processing software and WSxM 4.0 Beta 1.0 (Nanotec Electronica, S.L.) were used for image analysis.

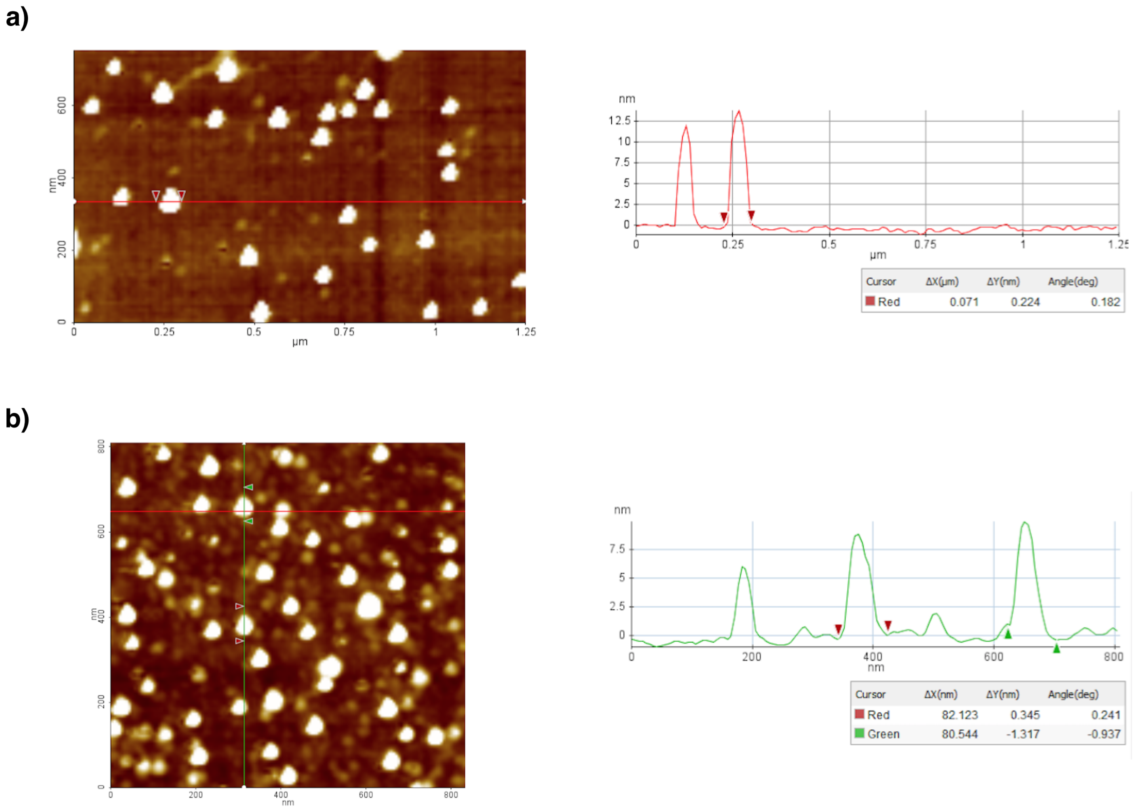

Figure S29: AFM images and height profile of : a) left-handed nanospheres, b) right-handed nanospheres.

6. Dynamic coordination and nanostructuration studies of Poly-2/Ba^{2+} using diiferent alcohols as cosolvents

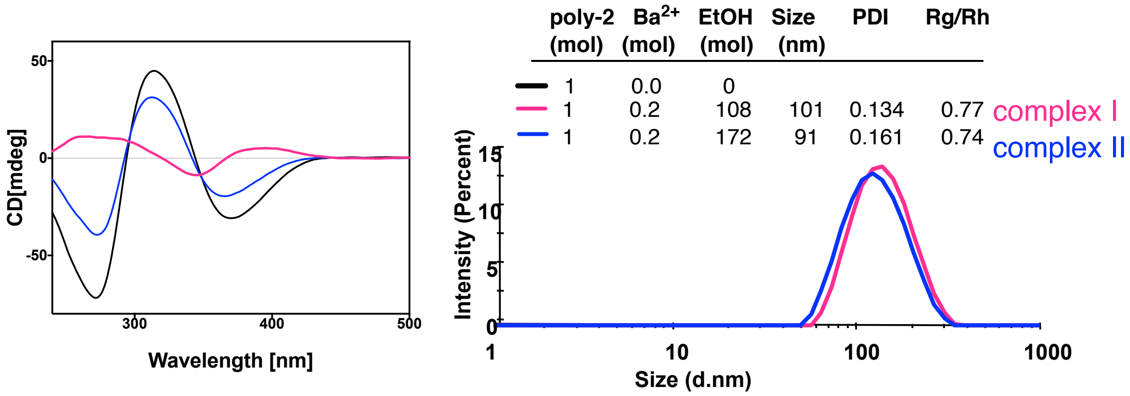

	poly-2 (mol)	Ba^{2+} (mol)	EtOH (mol)	Size (nm)	PDI	Rg/Rh	
—	1	0.0	0				
—	1	0.2	108	101	0.134	0.77	complex I
—	1	0.2	172	91	0.161	0.74	complex II

Figure S30. CD and DLS studies of a chloroform solution of poly-**2**/Ba^{2+} complex with different amounts of ethanol used as cosolvent to form complex I and complex II structures.

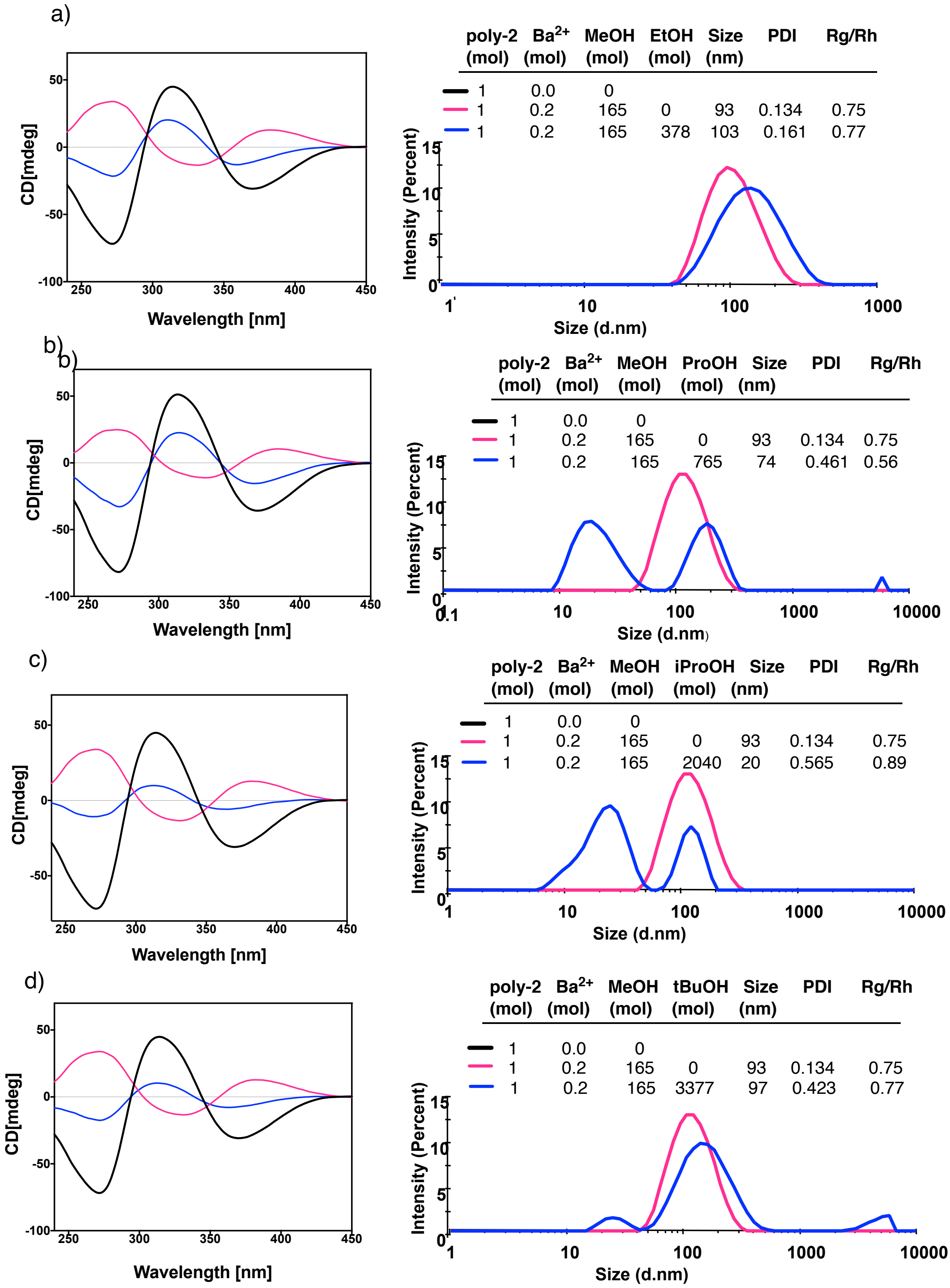

a)

	poly-2 (mol)	Ba^{2+} (mol)	MeOH (mol)	EtOH (mol)	Size (nm)	PDI	Rg/Rh
—	1	0.0	0				
—	1	0.2	165	0	93	0.134	0.75
—	1	0.2	165	378	103	0.161	0.77

b)

	poly-2 (mol)	Ba^{2+} (mol)	MeOH (mol)	ProOH (mol)	Size (nm)	PDI	Rg/Rh
—	1	0.0	0				
—	1	0.2	165	0	93	0.134	0.75
—	1	0.2	165	765	74	0.461	0.56

c)

	poly-2 (mol)	Ba^{2+} (mol)	MeOH (mol)	iProOH (mol)	Size (nm)	PDI	Rg/Rh
—	1	0.0	0				
—	1	0.2	165	0	93	0.134	0.75
—	1	0.2	165	2040	20	0.565	0.89

d)

	poly-2 (mol)	Ba^{2+} (mol)	MeOH (mol)	tBuOH (mol)	Size (nm)	PDI	Rg/Rh
—	1	0.0	0				
—	1	0.2	165	0	93	0.134	0.75
—	1	0.2	165	3377	97	0.423	0.77

Figure S31. CD and DLS studies of a poly-**2**/Ba^{2+}/MeOH system (complex I), titrated with different amounts of (a) ethanol, (b) propanol, (c) isopropanol and (d) tertbutanol used as cosolvent.

7. Supporting References

i) F. Freire, J. M. Seco, E. Quiñoá, R. Riguera, *Angew. Chem. Int. Ed.* 2011, **50**, 11692.